EVALUATION OF ANTIMICROBIAL AND ANTICANCER PROPERTIES USING AGAR DISC-DIFFUSION ANTIBIOTIC SUSCEPTIBILITY METHOD WITH CEO_2 NANOPARTICLES DOPANTS

Poornima N[1*], Sasikumar N[2], Dr. C Pandurangappa[3]

Abstract

Antimicrobial activity is the most important to inhibit the growth of bacteria and fungi infections, prevent the creation of microbial colonies, and destroy microorganisms. These have been widely used and greatly benefited the health-related quality of human life. However, the rapid emergence of antibiotic-resistant bacteria has created various problems with serious trouble for the medical community in measuring ionizing radiation exposure in dosimeter applications. Therefore, the use of doped nanoparticles as an alternative for measuring antimicrobial activity has been investigated. In this paper, the Agar disc-diffusion antibiotic susceptibility method is developed for antimicrobial activities analysis. The proposed technique uses the input of the samarium-doped, silver-doped, and Europium-doped CeO2 nanoparticles. Prepared samples are tested for measuring the antimicrobial activities against the ciprofloxacin bacteria and Itraconazole yeast or fungus by applying an Agar disc-diffusion antibiotic susceptibility method. In order to find the antibacterial and antifungal effects of the doped CeO2 nanoparticles, methanol is used as a control in the disc-diffusion susceptibility test. During the disc-diffusion process, the zone of inhibition is measured based on the compound on Clostridiumper fringens, Neisseria gonorrhoeae, Aspergillus flavus, and Candida albicans. In addition, minimum inhibitory activity is also measured and confirms that the doped CeO2 nanoparticles showed very good antibacterial and antifungal activity against the tested samples since their increased surface reactivity at the nano level. After that, the photoluminescence and thermoluminescence methods are analyzed for dosimeter applications. The radiation dosimetry involves measurement, calculation, and assessment of the quantity and quality of ionizing radiation exposed to and attenuated through the human body. The doped CeO2 nanoparticles are also associated with anticancer effects. While preserving the normal cells, these doped CeO2 nanoparticles applied for anticancer effects. The performance results indicate that the proposed method attains more efficiency in the antibacterial and antifungal effects as well as anticancer effects of doped CeO2 nanoparticles.

Keywords: Doped CeO_2 nanoparticles**, a**gar disc-diffusion antibiotic susceptibility method, photoluminescence, thermoluminescence method, anticancer effects analysis

[1*]Research Scholar, Research and Development Centre, Bharathiar University, Coimbatore, India, purnimaa.purnimaa@gmail.com
[1*]Assistant Professor, Department of Physics, Sir M. Visvesvaraya Institute of Technology, Bengaluru, India, purnimaa_phy@sirmvit.edu
[2]Assistant Professor, Department of Physics, Sir M. Visvesvaraya Institute of Technology, Bengaluru, India, sasikumarn7@gmail.com , sasikumar_phy@sirmvit.edu
[3]Associate Professor, Department of Physics, RNS Institute of Technology, Bengaluru, India, cpandu@gmail.com , hod.physics@rnsit.ac.in

***Corresponding Author:** Poornima N
*****Research Scholar, Research and Development Centre, Bharathiar University, Coimbatore, India, purnimaa.purnimaa@gmail.com
*****Assistant Professor, Department of Physics, Sir M. Visvesvaraya Institute of Technology, Bengaluru, India, purnimaa_phy@sirmvit.edu

DOI: 10.48047/ecb/2023.12.si10.0xyz

1. Introduction

Antibiotics or antimicrobials have been broadly utilized in a variety of fields like medicine, the food industry, agriculture, domestic animals, water healing for disease avoidance, pathogens suppression and etc. Therefore, the antibacterial efficiency of CeO2 NPs needs to improve in numerous applications. Several methods have been developed for antimicrobial activity analysis.

A rapid green precipitation method was developed in [1] for achieving high antimicrobial activity of cerium oxide nanoparticles by using leaf extract. However, the resulting nanoparticle was not effective for reliably applied in biomedical applications. An enhanced antibacterial property of green synthesized was obtained in [2] for cerium oxide nanoparticles through Agathosma betulina natural extract. However, the thermal thermoluminescence property was not analyzed.

The ZnSO4 doped CeO2 nanoparticles synthesis was developed in [3] using a chemical precipitation technique and then subjected to structural, optical, and antibacterial activity characterization analysis. However, ZnSO4 doped CeO2 nanoparticles provide a better antibacterial activity but the antifungal analysis was not performed. The antibacterial activities and MICs of CeO2 nanoparticles were analyzed in [4] against ESKAPE pathogens. But it failed to reveal the mechanism of action of these nanoparticles on ESKAPE pathogens. The antibacterial effect of cerium oxide nanoparticles was analyzed in [5] for achieving high antibacterial resistance. But the high antifungal resistance was not achieved. The antimicrobial activity of cerium oxide nanoparticles was analyzed in [6] for biomedical application.

The inhibitory activity of Fe-doped CeO2 nanoparticles was analyzed in [7] against pathogens. However, the long-term effect was not conducted to improve the antimicrobial effects. An antibacterial activity analysis was performed in [8] for Silver-doped cerium oxide nanoparticles against pathogenic bacteria. The antibacterial activity of cerium oxide nanoparticles with Gram-negative and Gram-positive foodborne pathogens was considered in [9]. Hydrothermal synthesis of samarium (Sm) doped cerium oxide (CeO2) nanoparticles was developed in [10] for analyzing the characterization of antibacterial activity.

1.1 Paper Contributions

From the analyses of existing work, novel method is developed with the following contributions.

- First, agar disc-diffusion antibiotic susceptibility method is developed for antimicrobial activity analysis of doped CeO_2 nanoparticles through the diameter of inhibition zone to find the susceptibility or resistance of bacteria and fungus.
- Then the photoluminescence with gamma radiation method is applied for analyzing the optical properties and identifying the peak intensity at a particular wavelength of light.
- After that, the Thermoluminescence dosimeter is developed for identifying the peak intensity based on radiation exposure according to the various temperature.
- The doped CeO2 nanoparticles are also used for evaluating the anticancer effects through the MTT assay analysis.
- Finally, performances of different characteristics are analyzed and discussed.

1.2 Paper organization

The paper is structured into various sections as follows. Section 2 reviews the related works of the antibacterial activity analysis. Section 3 provides a brief description of the different processes such as Agar disc-diffusion antibiotic susceptibility method, photoluminescence and thermoluminescence method for dosimeter applications. Section 4 describes the performance results and discussion of different characteristics of the doped CeO_2 nanoparticles. At last, Section 5 concludes the paper.

2. Related works

The preparation of CeO2 nanoparticles using egg white and examination of antibacterial effects of liquid and solid growth medium were analyzed in [11]. But it was not efficient to provide novel and cost-effective biomedical applications. The characterization of the antimicrobial effect of cerium oxide nanoparticles was synthesized in [12] by means of neem and ginger. A two-shape-CeO2 nanoparticles were synthesized in [13] for efficient antibacterial activity analysis. But it failed to attain many optimized and controlled outcomes.

Cerium-doped bioactive glasses were developed in [14] to apply a considerable antibacterial effect analysis. But doping with additional functionalization with drugs was not considered. Cerium oxide (CeO2) nanoparticles (NPs) were organized [15] through laser ablation in water at various laser energies for antibacterial and cytotoxic activities analysis. Antifungal activity of cerium oxide nanoparticles (CeNP) was

estimated in [16] against Candida albicans strains for clinical applications.

A Green synthesizes of silver-doped CeO2 nanoparticles was performed in [17] for effective photocatalysts and potential antibacterial agents. Green Synthesis of ciprofloxacin-overloaded Cerium Oxide Nanocarrier and its antibacterial activity were analyzed in [18]. Glycine-assisted hydrothermal synthesis was developed in [19] for pure and europium-doped CeO2 nanoparticles to analyze the antibacterial properties. However, the improved photodegradation performance and antibacterial activity were not identified. Gamma dose-dependent nanostructure optical properties of CeO2 thin films analysis were performed in [20]. But a strong and better radiation dosimeter property was not analyzed.

3. Methodology

Cerium oxide nanoparticles are currently being used as an antibacterial catalyst due to their small size; nanoparticles possess unique physical and chemical properties such as high magnetic moment, large conductivity, and extremely high complexation reactivity. Ceria nanoparticles prove the tremendous potential in antibacterial and antifungal activity against bacteria as well as fungus. The antibacterial activity of CeO2 nanoparticles has been investigated in bacteria and fungus. The doped CeO2 nanoparticles showed good antibacterial activity. In this paper, the agar disc-diffusion antibiotic susceptibility method is introduced for measuring the antibacterial and antifungal effects as well as anticancer effects of doped CeO2 nanoparticles.

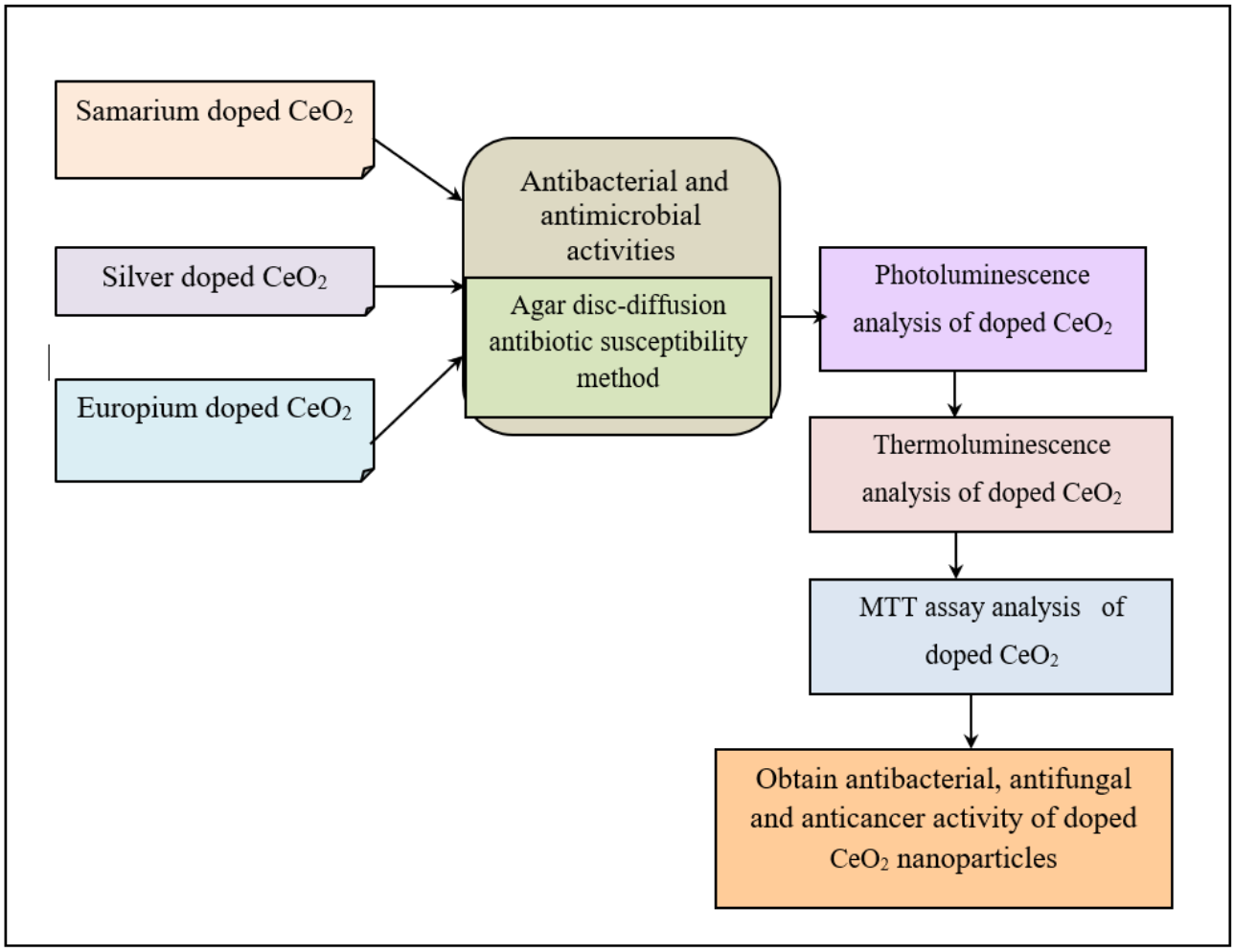

Figure 1 Architecture of the proposed method

Figure 1 illustrates an architecture diagram of the antibacterial and antimicrobial activities analysis of the proposed method that includes two different processes namely the Disc diffusion technique, with doped CeO2, and analyze the photoluminescence and thermoluminescence properties of doped CeO2 nanoparticles. The methodology considers the input as three types of CeO2 namely Samarium doped CeO2, Silver doped CeO2, Europium doped CeO2

First, the prepared Samarium-doped CeO2 samples, Silver-doped CeO2 samples, and Europium-doped CeO2 samples are considered as input for antibacterial and antifungal activities analysis. The Kirby Bauer disc-diffusion antibiotic susceptibility method is applied to identify the antibacterial and antifungal activities in the CeO2 NPs.

The proposed method considers the two antibiotics namely ciprofloxacin and Iitraconazole to quantify these antimicrobial effects. Ciprofloxacin is an antibiotic used to treat a number of bacterial infections. The Itraconazole is an antifungal medication applied to treat a number of fungal infections. Then the zone of Inhibition activity of the bacterial and fungal compound on Clostridiumperfringens, Neisseria gonorrhoeae, Aspergillus flavus, and Candida albicans was tested and measured. Based on the analyses, the diameter of the inhibition zone is estimated to find out the susceptibility of bacteria and fungus or yeast in the doped CeO2 nanoparticles.

Finally, the anticancer effects of the doped CeO2 nanoparticles are analyzed with the help of MTT assay analysis. The brief discussion of the Agar disc-diffusion antibiotic susceptibility method-based antimicrobial effects estimation is briefly explained in the following subsection.

3.1 Agar disc-diffusion antibiotic susceptibility method with Ciprofloxacin antibiotic

The agar disc-diffusion antibiotic susceptibility method is introduced for estimating the antimicrobial effects activity detection in the given doped CeO2 samples. The main purpose of the disk diffusion susceptibility test is to find bacteria and fungus infections to various antimicrobial compounds such as Ciprofloxacin and Itraconazole. The pathogenic organism is grown on Mueller-Hinton agar in the presence of various antimicrobial-infused filter paper disks.

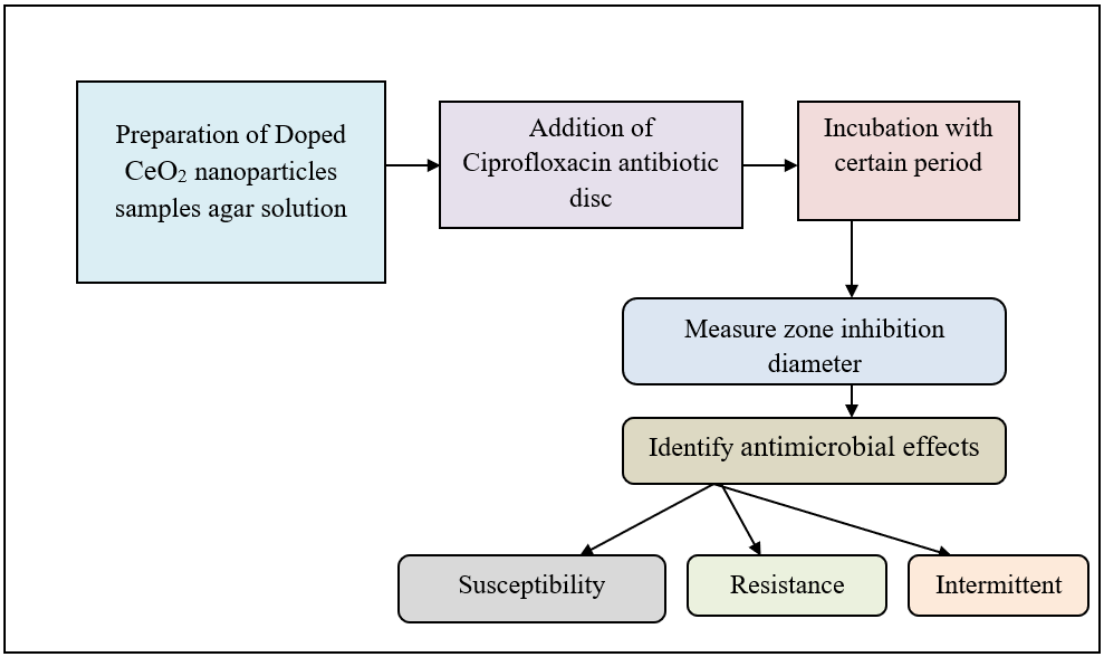

Figure2. Agar disc-diffusion antibiotic susceptibility method with Ciprofloxacin antibiotic

As shown in above figure 3, the process of agar disc-diffusion antibiotic susceptibility method with Ciprofloxacin antibiotic is developed for identifying the antifungal effects of the doped CeO_2 nanoparticles. The proposed disc-diffusion method consider the input of doped CeO_2,

3.1.1 Preparation of Samarium (Sm^{3+}) doped CeO_2 nanoparticles

The preparation process includes a Trisodium phosphate solution of 20 ml is added slowly drop wise to 60 ml of 0.1 M solution of cerium nitrate under magnetic stirring. The reaction mixture is under stable stirring and provides the white colloid. Then, the colloids are moved to the Teflon-coated autoclave container for performing the hydrothermal treatment at 180 ℃ for 15 hours. Then the autoclave container is cooled to room temperature. Finally, the impurities are removed widely and washed with double distilled water. As a result, the samarium-doped CeO2 nanoparticles are obtained for antimicrobial analysis. In this way, high-purity cerium and samarium salts are used to form a ceria-based solid solution.

3.1.2 Preparation of silver (Ag) doped CeO_2 nanoparticles

First, the solutions of the Cerium (III) nitrate hexahydrate [Ce $(NO_3)_3 \cdot 6H_2O$] and Silver nitrate [$AgNO_3$] salts are taken separately. After that, the solution of $AgNO_3$ is added drop by drop to Cerium (III) nitrate hexahydrate solution. Then the mixed solution was stirred at 80℃ for 6 hours. At last, clear gel-like honey is obtained. The obtained gel is dried in an oven at the temperature of 100◦C and calcined at 400 ℃ for 2 hours. Finally, silver-doped CeO_2 nanoparticles are obtained for antimicrobial analysis.

3.1.3 Preparation of Europium (Eu) doped CeO_2 nanoparticles

The solution of cerium (III) nitrate hexahydrate (Ce $(NO_3)_3 \cdot 6H_2O$) with the 0.130 and the 3 mol % of europium (III) nitrate hexahydrate (Eu $(NO_3)_3 \cdot 6H_2O$) are combined with the cerium nitrate transparent solution. Then the drop-wise addition of sodium hydroxide solution is added to the above mixture. This mixture is transferred to the 100 mL capacity of Teflon coated autoclave container at 150 ◦C for a 10 hrs reaction at 150 ◦C and the products are collected and washed several times with ethanol. Finally, in order to obtain the Eu doped CeO2 (ECDO) samples, the obtained solution is dried at 400 ◦C for 2 hours.

First, a Samarium-doped CeO2 nanoparticles agar solution is prepared using methanol as a control. An agar solution of the extract is prepared by dissolving 7g of nutrient agar with 100 mL of their respective solvents (distilled water and absolute methanol). The solution is warmed at 121℃ in the autoclave for 15 minutes. After that, a specific dose of Samarium doped CeO2 nanoparticles is added and properly mixed in nutrient agar solution is equally poured into six Petri dishes, and spent for 5 minutes to dry out.

After that, one bacterium from the Clostridiumper fringens, Neisseria gonorrhoeae is applied to the dried nutrient agar sample with the help of cotton scrub. The disc with a size of 6mm diameter infused with Ciprofloxacin antibiotic-loaded with 30 mg is placed in the center of the petri dish. Antibiotic-containing paper disks are then applied to the agar and the plate is incubated at 37℃ for 24 hours. If a Ciprofloxacin antibiotic stops the bacteria from growing or kills the bacteria, there is an area around the disk where the bacteria have not developed to be visible. This is called a zone of inhibition. The diameter of the inhibition zone is measured by means of a Vernier caliper to find the susceptibility or resistance of bacteria to Samarium-doped CeO2 nanoparticles. Based on the diameter of inhibition, the susceptibility of bacteria or fungus is determined as susceptible, resistant, and intermediate.

Whereas, the Sm3+ doped CeO2 nanoparticles provide a better antibacterial activity. The result obtained from the antibacterial analysis reveals that the bacteria-killing efficiency of Sm- CeO2 significantly increased by increasing the concentration of Sm3+ dopant.

In this way, antimicrobial effects are determined by applying the silver-doped and Europium-doped CeO2 nanoparticles with the Ciprofloxacin antibiotic. Therefore, the minimum diameter of the zone of inhibitory activity confirms that the doped CeO2 nanoparticles showed very good antibacterial activity against the bacteria-tested samples.

3.2 Agar disc-diffusion antibiotic susceptibility method with Itraconazole antibiotic

The agar disc-diffusion antibiotic susceptibility method is introduced for estimating the antimicrobial activity detection of the given doped CeO2 samples with Itraconazole antibiotic. Itraconazole is employed to treat a variety of fungal infections. The agar disc-diffusion antibiotic susceptibility method is used to determine the anti-microbial activity against fungal infections. In addition, the proposed disc-diffusion method is to quantify the ability of antibiotics to reduce fungus growth.

An assessment of studies of biologically active nanoparticles provides management for the synthesis of cerium oxide nanoparticles with the aim of developing new antibiotics or antifungals to fight against bacteria or fungus. This article focuses on the physicochemical properties of doped cerium oxide nanoparticles (CeNPs) with antimicrobial activity with Itraconazole antibiotic.

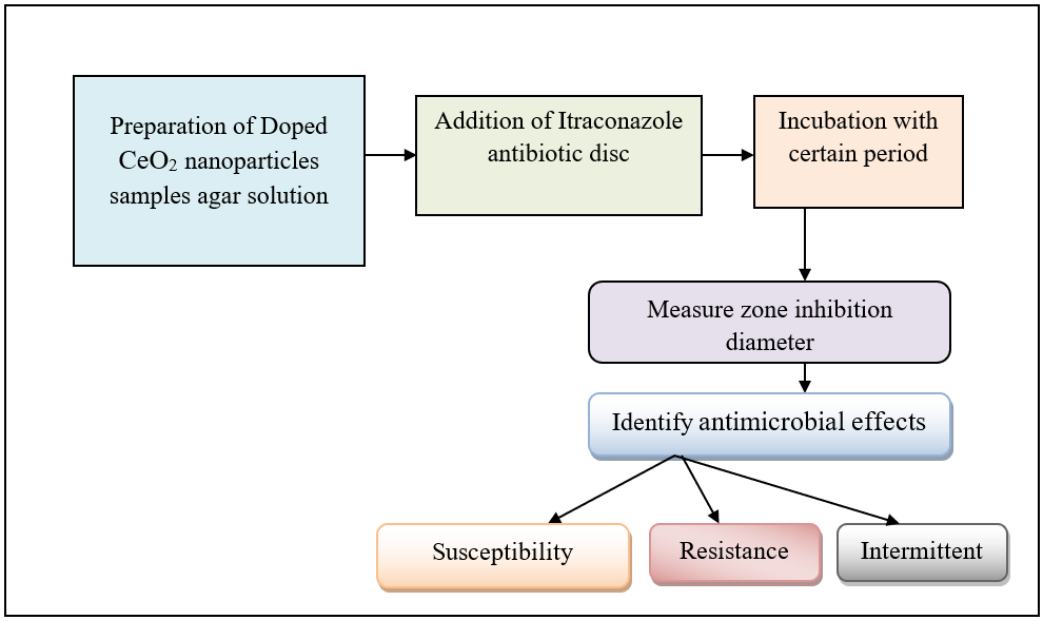

Figure 3. Agar disc-diffusion antibiotic susceptibility method with Itraconazole Antibiotic disc

As shown in above figure 2, the process of the Agar disc-diffusion antibiotic susceptibility method with Itraconazole antibiotic is constructed for identifying the antimicrobial effects of the doped CeO_2 nanoparticles. The proposed diffusion method uses the input of the samarium doped CeO_2, silver doped CeO_2, and europium doped CeO_2 nanoparticles solution for antimicrobial effects analysis of doped CeO2 nanoparticles.

First, Samarium-doped CeO_2 nanoparticles agar solution is taken as input and using methanol as a control. An agar solution of the extract is prepared by dissolving 7g of nutrient agar with 100 mL of their respective solvents (distilled water and absolute methanol). The solution is warmed at 121℃ in an autoclave for 15 minutes. After that, a particular dose of samarium doped CeO_2 nanoparticles is added drop by a drop manner and properly mixed in nutrient agar solution is equally poured into six Petri dishes and spent for 5 minutes to dry out.

After that, one fungus from the Aspergillus flavus and Candida albicans is applied to the dried nutrient agar sample with help of cotton scrub. Then the disc with a size of 6mm diameter was infused with Itraconazole antibiotic used in a concentration range from 0.016 to 8 mg/liter in the center of the petri dish. Antibiotic-containing paper disks are then applied to the agar and the plate is incubated at 37℃ for 24 hours. If an Itraconazole antibiotic stops the fungus from growing or kills the fungus, there is an area around the disk where the fungus has not developed to be visible. This is called a zone of inhibition. Finally, the diameter of the inhibition zone is measured with the help of a Vernier caliper to find the susceptibility of bacteria for samarium-doped CeO2 nanoparticles. Based on the diameter of estimation, the susceptibility of fungus is determined as susceptible, resistant, and intermittent.

In this way, antifungal effects are determined by applying the silver-doped and Europium-doped CeO2 nanoparticles with the Itraconazole antibiotic. Therefore, the minimum diameter of the zone of inhibitory activity confirms that the doped CeO2 nanoparticles provide better antifungal activity against the fungus-tested samples.

3.2 Photoluminescence gamma dose dosimeter method for doped CeO2 nanoparticles

Photoluminescence dosimetry is the process of quantifying the absorbed dose of ionizing radiation by means of detectors that show the luminescence. This dosimeter is employed as an extremely sensitive and cost-effective in ultra-low-dose environment to identify the radiation properties of doped CeO_2 nanoparticles on the optical properties. The photoluminescence (PL) emission spectra of the doped CeO_2 nanoparticles measured at an excitation wavelength. First, a monochromatic light, source typically a laser or UV light source is used to stimulate the doped CeO_2 nanoparticles. Photoluminescence process is depending on the light interacts with the doped CeO_2 sample. This method occurs when the light source is absorbed and emitted at a range of longer wavelengths.

The laser light is passed onto doped CeO_2 nanoparticles, the electrons inside the samples moved from low energy into higher energy excited states. This only takes places when the energy of the photon or light is greater than the wide band gap energy levels normally ranged from 3.2 to 3.5 eV.

After a few nanoseconds the electron in excited states moved down to ground state and releases and emits the absorbed energy in the form of a photon which called as relaxation. This spontaneous emission of the photon due to optical excitation is called photoluminescence.

The emitted light is explored through the spectrometer to obtain the structural information about the doped CeO_2 nanoparticles. The observed intensity curve indicates that the linearly increased while increasing the wavelength of the light. But the peak intensity is identified at a particular wavelength of light with different gamma doses up to 100 kGy for dosimeter application. After reaches the peak intensity at particular wavelength, the intensity gets reduced with increasing gamma exposed dose.

3.3 Thermoluminescence dosimeter method for CeO_2 nanoparticles

Thermoluminescence dosimeter (TLD) is a passive radiation detection that helps to measure the ionizing radiation exposure by estimating the intensity of light emitted from doped CeO_2 nanoparticles in the detector when heated. The peak intensity of light is emitted based on radiation exposure.

In order to improve thermoluminescence property, the CeO_2 nanoparticles is doped with Sm^{3+}, Ag and Eu. Thermoluminescence is defined as the emission of light intensity is obtained by the thermal recombination of previously entrapped electrons and holes pairs. Thermoluminescence spectroscopy refers to an excitation spectroscopy in which emission of light from CeO_2 nanoparticles irradiated with radiations is generated by heating.

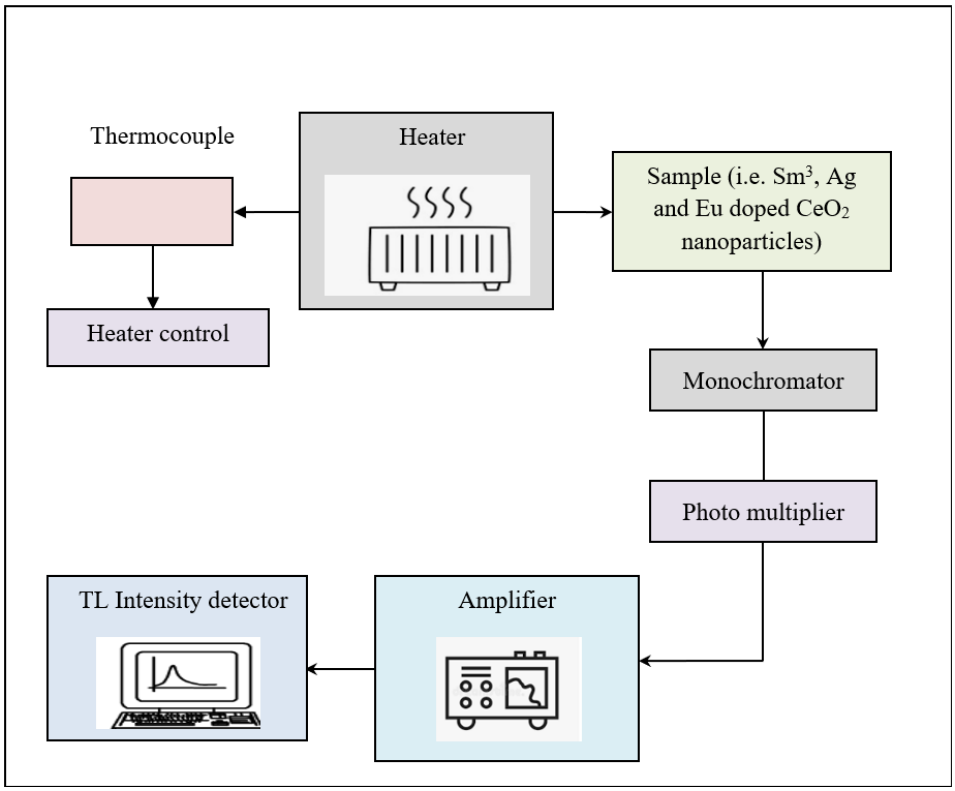

Figure 4 Block diagram of Thermoluminescence dosimeter set-up

As shown in above figure 4, the process of Thermoluminescence dosimeter setup is constructed for identifying the thermal property of the doped CeO_2 nanoparticles. First, the heater typically is used to emit heat with different Celsius (℃). Then the heat is applied on the sample (i.e. Sm^3, Ag and Eu doped CeO_2 nanoparticles), it is absorbed and initiates the excess heat energy. This excess amount of energy is dissipated through the emission of heat, which is called as Thermoluminescence process.

When the thermo-luminescent materials are exposed to ionizing radiations like gamma dosimeter, the system absorbs energy and changes from stability to a metastable state. This change is occurred by the means of transit of electrons from

the valence band to the conduction band resulting it free electrons and holes trap pairs are generated. These free charge carriers move freely and may get trapped at the defect sites thereby leading the storing of irradiation energy by doped CeO_2 nanoparticles. These CeO2 nanoparticles when heated may release the stored charge subsequently the relaxation of the system back to the equilibrium. The temperature at which the charge carriers are released from trap based on upon energy difference of trap depths and conduction/valence band. The released electron from conduction band to ground state in recombination produces a photon in the form of heat energy. The heat emission process of Thermoluminescence dosimeter method is shown in figure 5(a) (b).

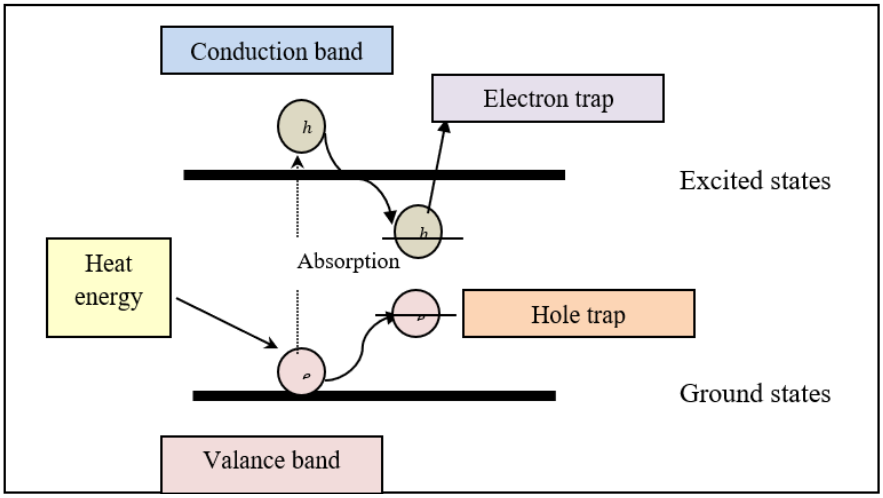

5(a)

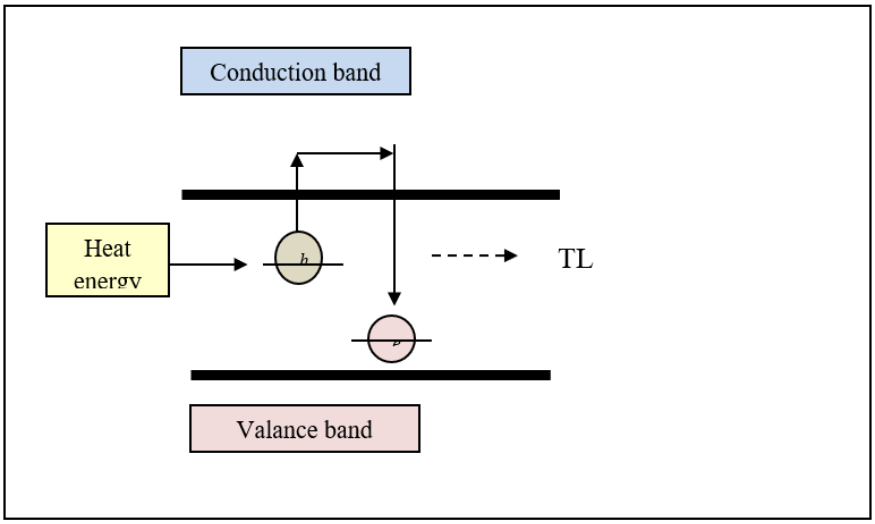

Figure 5 (b) Schematic diagram of TL emission process

Figure 5 illustrates the simple model of the thermoluminescence process. By applying a thermoluminescence method, there are two states are employed for light emission process such as higher energy state and lower energy state. The higher energy state is called as excited states whereas the lower energy states are called as ground states. The observed TL intensity curve indicates that the linearly increased while increasing the temperature of the heater. But the peak intensity is identified at a particular temperature. After reaches the peak value, then the intensity gets reduced linearly while increasing the temperature.

3.4 Evaluation of anticancer effects of doped CeO_2 nanoparticles using MTT analysis

In this section, anticancer activity is analyzed using biocompatible CeO_2 nanoparticles synthesized by the two types of plants such as Centella Asiatica (CA) and Indigofera Tinctoria (IT). In the synthesis process, the aqueous leaf extracts of Centella Asiatica and Indigofera tinctoria plant is called as biofuels.

The anticancer activity of the dopant CeO_2 nanoparticle is performed by applying a MTT assay. It is a colorimetric assay which done to assess the cell viability. With the development of MTT analysis, the diverse abilities of dopant CeO_2 nanoparticle have encouraged as a therapeutic agent to treat cancer in human cells. A 25000 cells/well are started in a 96-well plate. Dimethyl sulfoxide solution is used as the solvent control. After 24 hours of incubation at 37°C, dopant CeO_2 nanoparticle with different concentrations 0, 15.6, 31.2, 62.5, 125, and 250 µg/mL are incubated for another 48 hours. Then the 20 µl of 3-(4, 5-di-methylthiazol-2-yl)-2, 5-diphenyl-2H-tetrazolium bromide MTT solution is added to each well and the plate is covered with aluminum foil and incubated for 4 h at 37°C. After incubation with MTT reagent, the medium is removed from the wells. Then the dimethyl sulfoxide is added to each well. After shaking the plates for 3 minutes absorbance was recorded at 570 nm (measurement) and 630 nm (reference). Therefore, percentage inhibition is calculated using the formula:

$$I = \left(1 - \frac{a_s}{a_c}\right) * 100 \quad (1)$$

Where, percentage of inhibition, a_s denotes an absorbance presence of test sample, a_s indicates a absorbance of control.

4. RESULTS AND PERFORMANCE ANALYSIS

In this section, performance analysis of doped CeO_2 nanoparticles is analyzed with different metrics such as antibiotic-resistance profile, Photoluminescence intensity, Thermoluminescence intensity, XRD data graph calculation, SEM, TEM, FE- SEM, XPS and percentage of inhibition, Cell viability test by MTT assay , anticancer activity of colony-forming assay, GCMS analysis of leaf extracts Indigoferra tinctoria and Centella Asiatica, LC–MS analysis of leaf extracts using Centella Asiatica and Indigoferra tinctoria**.** The performance are analyzed with the help of graphical illustration.

4.1 Impact of the antibiotic-resistance pofile

Antimicrobial analysis with doped CeO_2 nanoparticles is analyzed with different test bacteria and fuungus. Inhibition Zone test is performed to determine the susceptibility or resistance of pathogenic bacteria or fungus to antibiotic agents. In comparison to other laboratory test methods, the zone of Inhibition test is an efective and fast way to determine antibiotic activity.

Table 1 Antibiotic-resistance profile for doped CeO_2 nanoparticles with Ciprofloxacin

Test bacteria	**Inhibition Zone (mm)**		
	Ciprofloxacin+ Sm^{3+} doped CeO_2	**Ciprofloxacin+ Ag doped CeO_2**	**Ciprofloxacin+ Eu doped CeO_2**
Clostridiumper fringens	10.00 (R)	9.00 (R)	14.00 (R)
Neisseria gonorrhoeae	11.00 (R)	13.00 (R)	15.00 (R)
Acinetobacter baumannii	9.50 (R)	14.50 (R)	14.50 (R)
Enterococcus faecium	9.00 (R)	17.00 (R)	12.00 (R)
Klebsiella Pneumonia	13.00(R)	11.00(R)	21.00 (R)

Table 1 describes the performance results of the antibiotic-resistance profile of antibacterial effects of the doped CeO_2 nanoparticles. In this analysis, the Inhibition Zone is measured for ciprofloxacin antibiotic with Sm^3 doped CeO_2, Ag doped CeO_2, Eu doped CeO_2. On order to perform the antibacterial effects, the test bacteria are considered as Clostridiumper fringens , Neisseria gonorrhoeae, Acinetobacter baumannii, Enterococcus faecium, Klebsiella Pneumonia. From the analysis, the observed results of the inhibition zone indicate that the antibacterial effects of the doped CeO_2 nanoparticles are resistance (i.e. R) to bacterial infections.

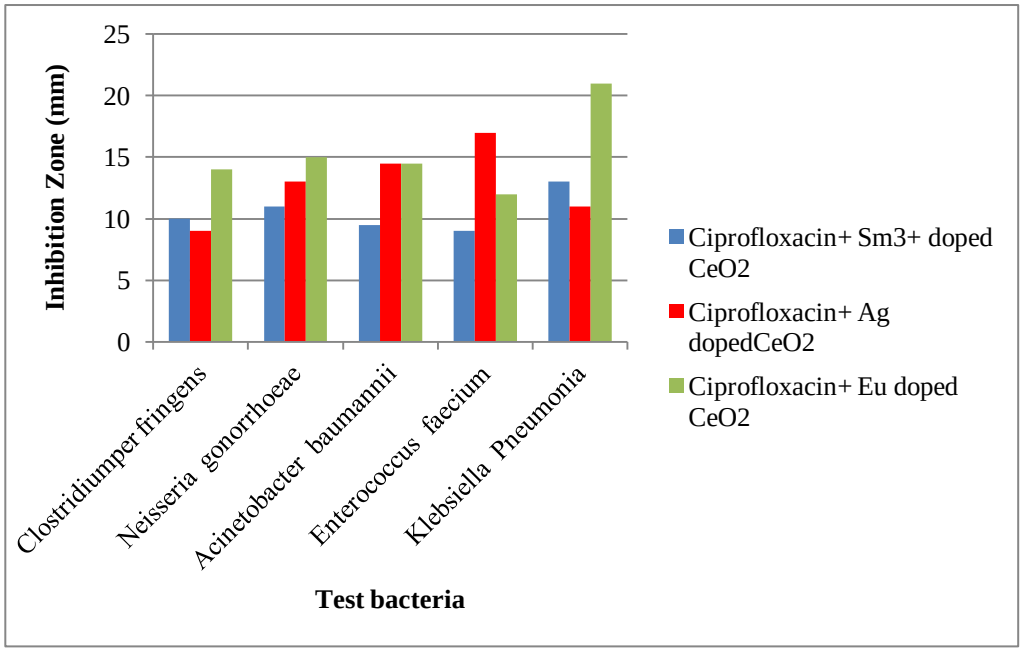

Figure 6. Antibiotic-resistance profile pattern with doped CeO_2 nanoparticles with Ciprofloxacin

From the tabulated results, the performance of is antibiotic-resistance profile pattern in the graphical format. In this validation, the performance of the antibiotic-resistance profile pattern technique gets increased. The reason is the technique uses the agar disc-diffusion antibiotic susceptibility method. The method is applied for analyzing the inhibition zone of the disc. Based on the analysis, the doped CeO_2 nanoparticles is resistance to the bacterial infections.

The zone inhibition using agar disc-diffusion antibiotic susceptibility method with different test bacteria images are shown in figure 7.

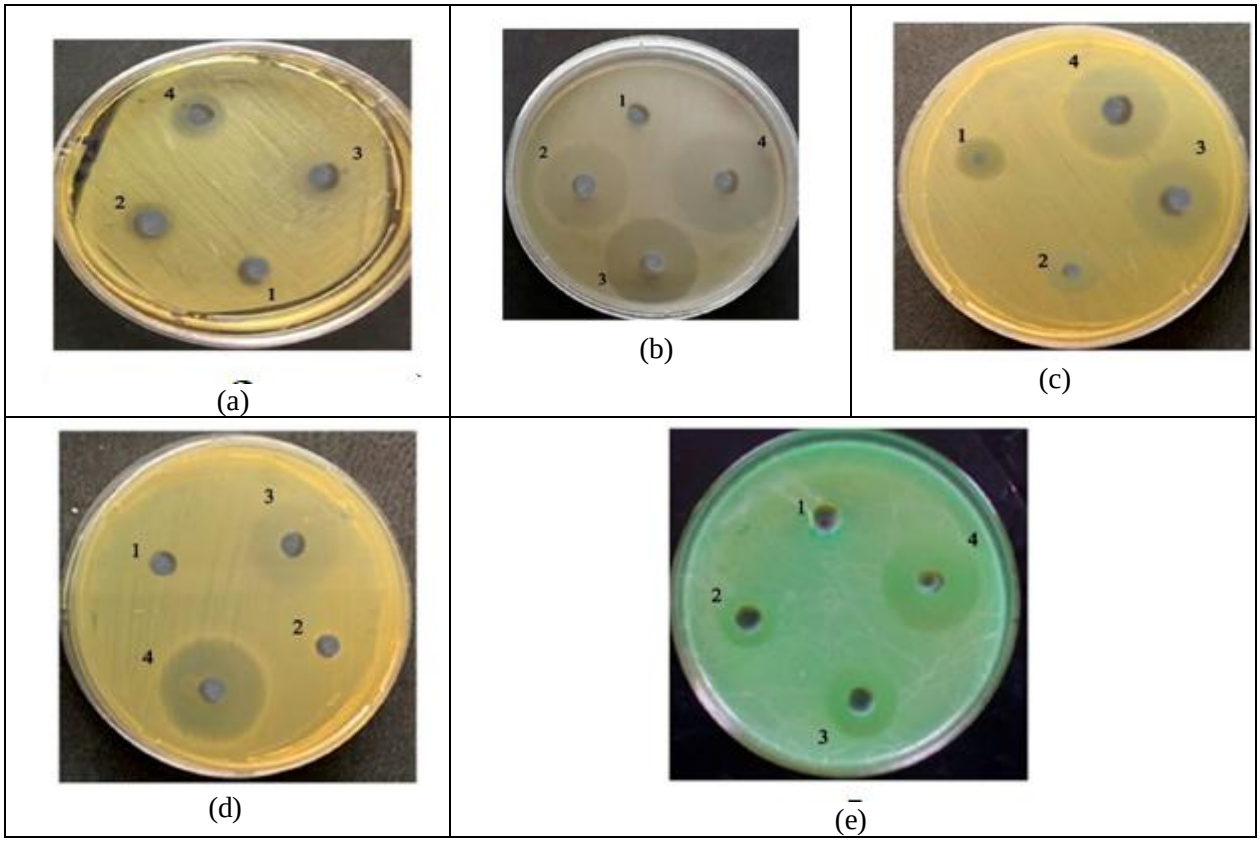

Figure 7 Antibacterial activities of CeO_2 nanoparticles (a) Enterococcus faecium (b) Clostridiumper fringens (c) Klebsiella Pneumonia (d) Acinetobacter baumannii (e) Neisseria gonorrhoeae

Table 2 Antibiotic-resistance pofile for doped CeO2 nanoparticles with Ciprofloxacin

Test fungus	**Inhibition Zone (mm)**		
	Iitraconazole + Sm^{3+} doped CeO_2	**Iitraconazole + Ag doped CeO_2**	**Iitraconazole + Eu doped CeO_2**
Aspergillus flavus	12.00 (R)	15.00 (R)	17.00 (R)
Candida albicans	11.00 (R)	16.00 (R)	18.00 (R)
Aspergillus terreus	14.00(R)	17.00(R)	20.00(R)
Aspergillus niger	14.50(R)	18.50(R)	21.00(R)
Fusarium	15.00(R)	19.00(R)	21.50(R)

Table 2 describes the performance results of the antibiotic-resistance profile of antibacterial effects of the doped CeO_2 nanoparticles. In this analysis, the Inhibition Zone is estimated for Iitraconazole antibiotic by means of Sm^3 doped CeO_2, Ag doped CeO_2, Eu doped CeO_2. On order to perform the antifungal effects, the test fungus is considered as Aspergillus flavus, Candida albicans, Aspergillus terreus, Aspergillus niger and Fusarium. From the analysis, the observed results of the Inhibition zone indicate that the antifungal effects of the doped CeO_2 nanoparticles are resistance (i.e., R) to fungus infections.

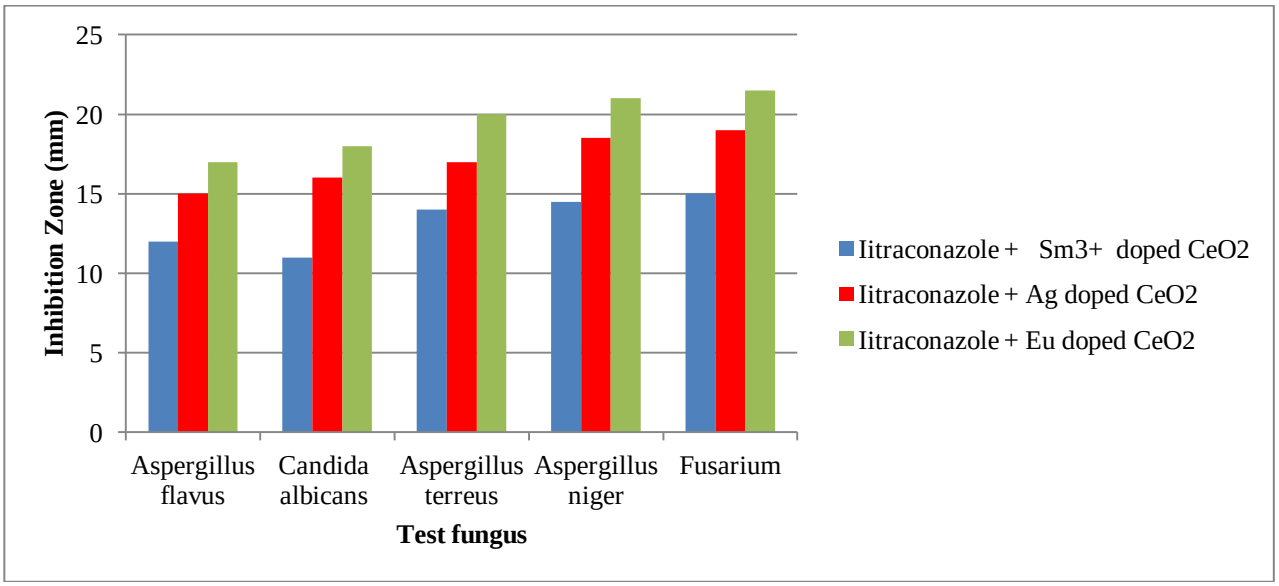

Figure 8. Antibiotic-resistance profile pattern with doped CeO_2 nanoparticles with Iitraconazole antibiotic

The performance of is antibiotic-resistance profile pattern are illusstrated in the graphical format as shown in figure 8. From the analysis, performance of the antibiotic-resistance profile pattern gets increased for doped CeO_2 nanoparticles. The reason behind that the agar disc-diffusion antibiotic susceptibility method is applied for effective an antifungal effect analysis. The method is also used for analyzing the inhibition zone of the disc and identifies the bacterial infections.

The zone inhibition using agar disc-diffusion antibiotic susceptibility method with different test fungus images are shown in figure 9.

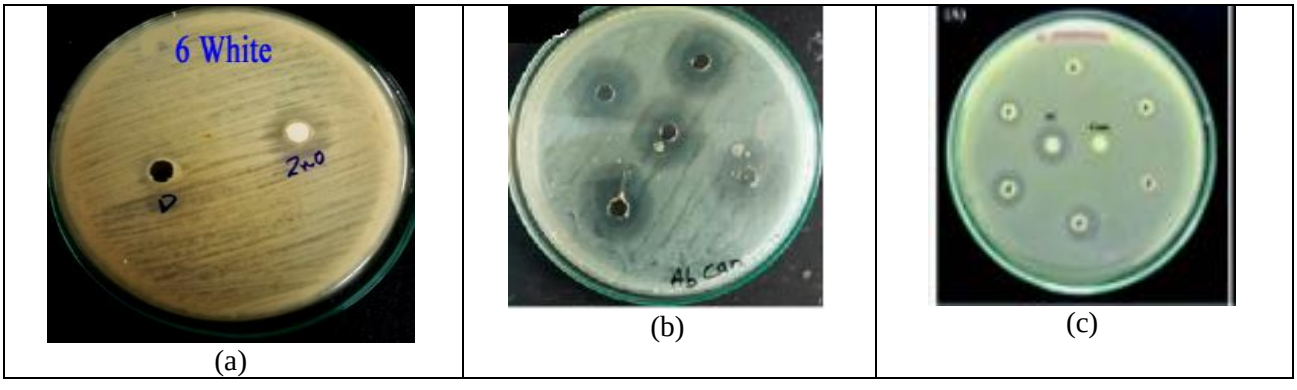

(a) (b) (c)

(d)

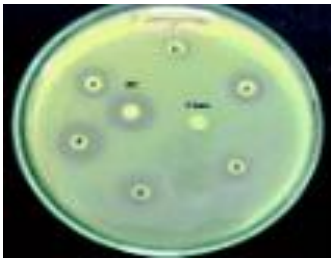

(e)

Figure 9 Antifungal activities of CeO_2 nanoparticles (a) Aspergillus flavus (b) Candida albicans (c) Aspergillus terreus (d) Aspergillus niger (e) Fusarium

4.2 Impact of Photoluminescence intensity with dosimeter application

Photoluminescence intensity is the measure of emitted light intensity with a function of wavelength in the optical spectrometer for gamma radiation dosimeter. The intensity of emitted light is measured with respect to wavelength in nanometer (nm). The Photoluminescence intensity is measured in terms of absorption unit (a.u). The Photoluminescence intensity for gamma radiation dosimeter is analyzed for Sm^{3+} doped CeO_2, Ag doped CeO_2 and Eu doped CeO_2.

The emitted intensity of photon or light is measured as follows,

$$E_{pt} = \frac{h_{pt} * C_{pt}}{\lambda_{pt}} \qquad (2)$$

Where, E_{pt} denotes an emitted intensity of photon, h_{pt} denotes a Planck's constant $(6.626 * 10^{-34} Js)$, C_{pt} denotes a speed of the photon or light $(3 * 10^8 m/s)$, λ_{pt} indicates a wavelength of the photon or light in meter.

- Let us consider, h_{pt} denotes a Planck's constant $(6.626 * 10^{-34} Js)$, C_{pt} denotes a speed of the photon or light $(3 * 10^8 m/s)$, $\lambda_{pt} = 400nm$. The emitted intensity of photon or light is calculated as,

$$E_{pt} = \frac{(6.6.2610^{-34}) * (3 * 10^8)}{400} = 3.10eV \qquad (3)$$

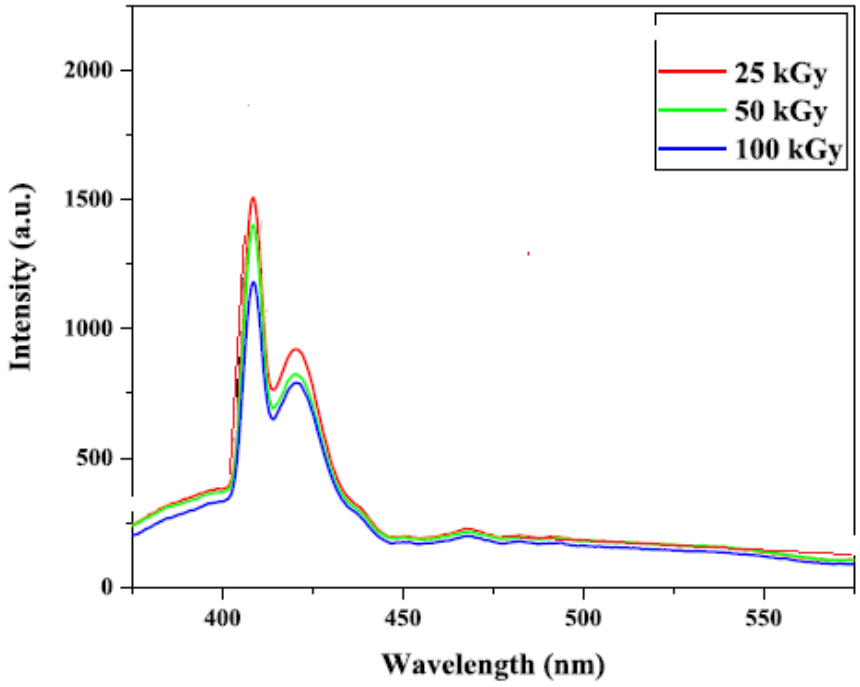

Figure 10 Photoluminescence intensity for gamma radiation dosimeter with Sm^{3+} doped CeO_2

Figure 10 illustrates the photoluminescence (PL) intensity to analyze light emission properties of CeO_2 nanostructure thin films. To obtain a deeper understanding of gamma irradiation effects within the CeO_2 nanostructure films and its optical response, PL spectra have been measured at room

temperature with a peak wavelength of 415 nm. Then the intensity of peaks gradually decreased with increasing gamma exposed dose from 25kGy, 50kGy and 100 kGy.

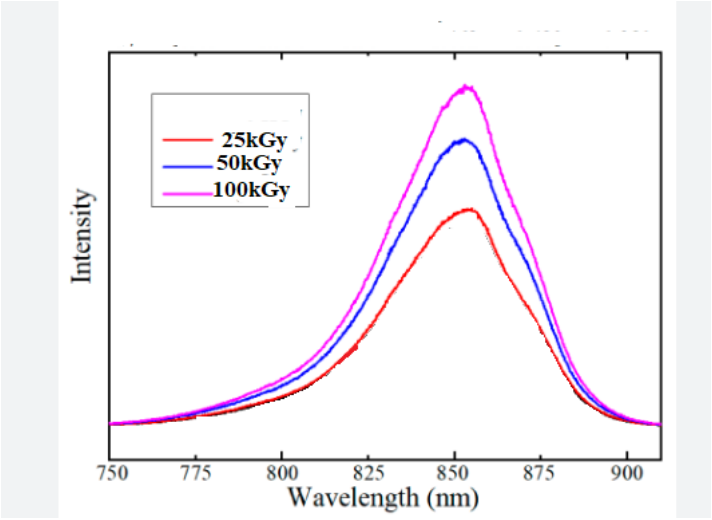

Figure 11 Photoluminescence intensity for gamma radiation dosimeter with Ag doped CeO_2

Figure 11 illustrates the photoluminescence (PL) intensity properties of Ag doped CeO_2 nanostructure thin film for gamma radiation dosimeter application. To obtain a deeper understanding of gamma irradiation effects within the CeO_2 nanostructure films and its optical response, PL intensity is obtained at the peak wavelength of 860 nm. Then the intensity of peaks gradually decreased with increasing gamma exposed dose from 25kGy, 50kGy and 100 kGy.

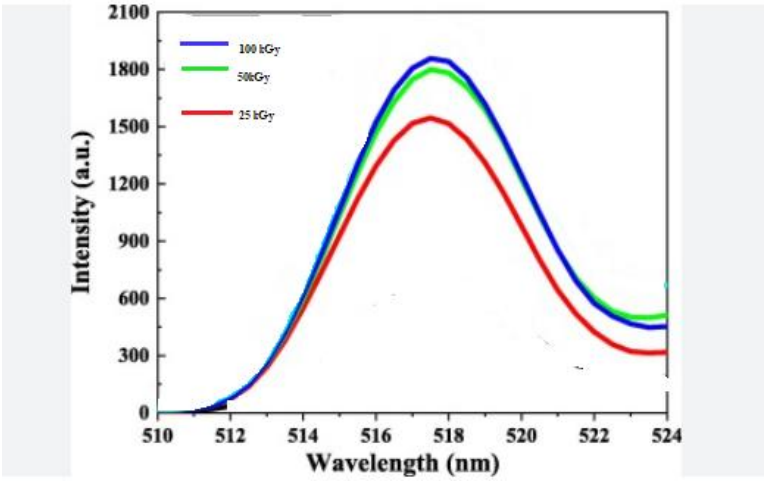

Figure 12 Photoluminescence intensity for gamma radiation dosimeter with Eu doped CeO_2

Figure 12 illustrates the photoluminescence (PL) intensity properties of Eu doped CeO_2 nanostructure thin film for gamma radiation dosimeter application. To obtain gamma irradiation effects of the CeO_2 nanostructure films and PL intensity is obtained at the peak wavelength of 518nm. Then the intensity of peaks gradually decreased with gamma exposed dose from 25kGy, 50kGy and 100 kGy.

4.3 Impact of thermoluminescence intensity with dosimeter application

Thermoluminescence (TL) intensity is an extensive method used for ionizing radiation dosimetry purposes, since the energy absorbed during irradiation and the TL intensity on heating are proportional to the radiation flux (doses).
The Thermoluminescence (TL) intensity is computed using following formula,

$$\text{TL intensity} = \text{N S} \exp\left(\frac{Energy}{k*Temp}\right) \quad (4)$$

Where, N denotes a the trap population density, S denotes a frequency factor for interactions with the trapped charge, $Energy$ denotes a trap depth or activation energy, which is the energy needed

to release an electron from the trap into the conduction band , k = Boltzmann's constant = $8.617 \times 10^{-5}\ eV$

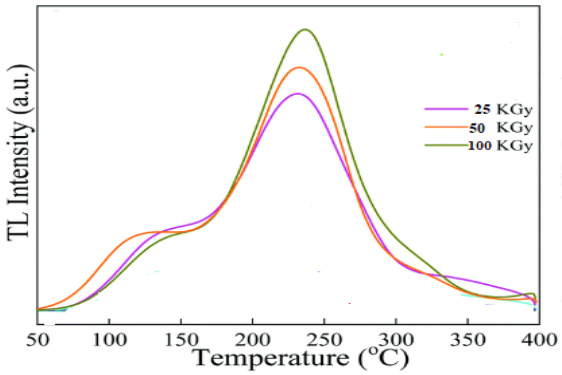

Figure 13 TL intensity for gamma radiation dosimeter with Sm^{3+} doped CeO_2

Figure 13 illustrates the performance analysis of TL intensity properties of Sm^{3+} doped CeO_2 thin film for gamma radiation dosimeter application. TL intensity is measured based on the different temperature from 50℃ to 400℃. The intensity of peaks temperature is obtained at 230℃

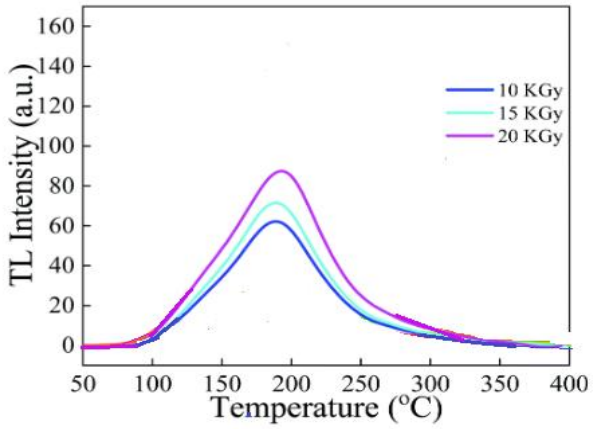

Figure 14 TL intensity for gamma radiation dosimeter with Ag doped CeO_2

Figure 14 illustrates the performance analysis of TL intensity properties of Ag doped CeO_2 thin film for gamma radiation dosimeter application. TL intensity is measured based on the different temperature from 50℃ to 400℃. The intensity of peaks temperature is obtained at 190℃.

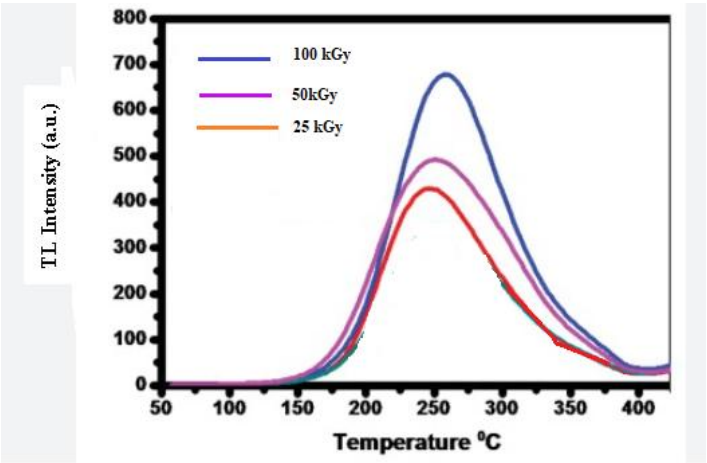

Figure 15 TL intensity for gamma radiation dosimeter with Eu doped CeO_2

Figure 15 illustrates the performance analysis of TL intensity properties of Eu doped CeO_2 nanoparticles for gamma radiation dosimeter. TL intensity is measured based on the different temperature from 50℃ to 400℃. The intensity of peaks temperature is obtained at 250℃.

4.4 X-ray diffraction (XRD) for doped CeO2 nanoparticles

X-ray diffraction (XRD) characteristics of doped CeO_2 nanoparticles are performed in this section. X-ray diffraction analysis (XRD) is a method used in nanotechnology to determine the crystallographic size of doped CeO_2 nanoparticles.

The crystallite size using XRD pattern is calculated as follows,

$$crystallite\ size\ \ (\mathrm{S}) = \frac{k*\lambda_{Xray}}{b*\cos\theta} \quad (5)$$

Where, k denotes a constant depending on the crystallite size, λ_{Xray} denotes a wavelength of $X-ray$, b denotes a full width half maximum in radians, θ denotes a peak position in degree.

Crystallite size of Sm^{3+} doped CeO_2

- Let us consider$k = 0.94$, $\lambda_{Xray} = 1.5406\,\dot{A}$, $b = 0.33mm$, $2\theta = 28degree$ with fist peak position (111)

$$crystallite\ size\ \ (\mathrm{S}) = \frac{0.94 * 1.5406}{0.33 * \cos\ (28)} = 259.03nm$$

Crystallite size of Ag doped CeO_2

- Let us consider$k = 0.94$, $\lambda_{Xray} = 1.5406\,\dot{A}$, $b = 0.31mm$, $2\theta = 28degree$ with fist peak position (111)

$$crystallite\ size\ \ (\mathrm{S}) = \frac{0.94 * 1.5406}{0.31 * \cos\ (28)} = 275.75nm$$

Crystallite size of Eu doped CeO_2

Let us consider$k = 0.94$, $\lambda_{Xray} = 1.5406\,\dot{A}$, $b = 0.3mm$, $2\theta = 28degree$ with fist peak position (111)

$$crystallite\ size\ \ (\mathrm{S}) = \frac{0.94 * 1.5406}{0.3 * \cos\ (28)} = 284.94nm$$

Table 3 intensity versus angle

$2\theta\ (degree)$	**Intensity (a.u)**			
	Undoped	**Sm^{3+} doped CeO_2**	**Ag doped CeO_2**	**Eu doped CeO_2**
10	50	240	170	100
20	50	240	170	100
30	50	240	170	100
40	50	240	170	100
50	50	240	170	100
60	52	242	172	102
70	51	241	171	101
80	50	240	170	100

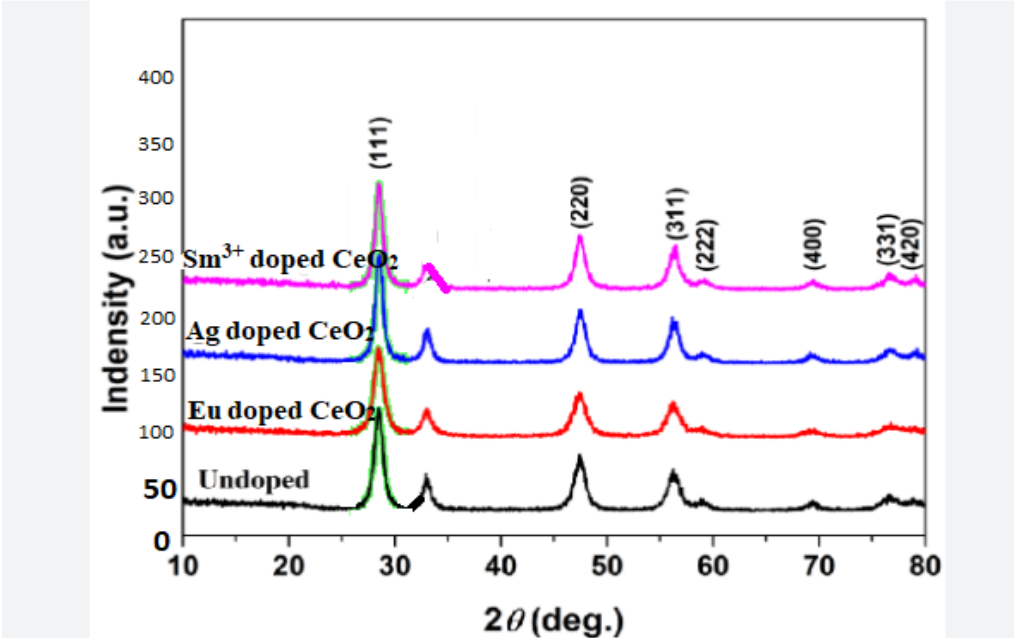

Figure 16 X-ray diffraction patterns of doped CeO_2-NPs

Figure 16 reveals the performance of X-ray diffraction patterns using doped CeO_2-NPs. As shown in the above graph, the vertical axis represents intensity in absorption unit (A.U) and the horizontal axis represents the diffraction angle in degrees. As shown in the graph, the intensity value of the Sm^{3+} doped CeO_2, Ag doped CeO_2, Eu doped CeO_2 and undoped are represented by pink color, blue color, red color and black color respectively. Therefore, an X-ray diffraction pattern of the doped CeO_2 is used for cardio myoblast hypertrophy treatment in the biomedical applications.

4.5 Scanning electron microscopy (SEM)

To analyze the effect of doped CeO_2 -NPs on the biofilm structural design of test bacteria, a Scanning Electron Microscopic (SEM) assessment of bacterial bio-films is performed.

In order to calculate the doped CeO_2-NPs particle with spherical structure using SEM assessment, first the diameters of the each spheres is measured based on the surface area of the particles.

$$D = 2 * \sqrt{\frac{Area}{\pi}} \quad (6)$$

Where, D denotes a diameter of the particle in nanometer. After calculating the diameter, the mean of the all the particles are computed.

$$M = \frac{\sum D}{n} \quad (7)$$

Where, M denotes a mean, $\sum D$ denotes a sum of the entire spheres diameter, n denotes a number of spheres in the given SEM image. Finally, mean of all the entire spheres is a size of the CeO_2-NPs particle.

Table 4 (a) example calculation of Sm^{3+} doped CeO_2 nanoparticles crystallite size

Number of spheres in SEM image	Diameter of spheres in SEM image (nm)
1	55
2	25
3	35
4	45
5	55
6	60
7	45
8	55
9	75
10	96
Average mean	54.6

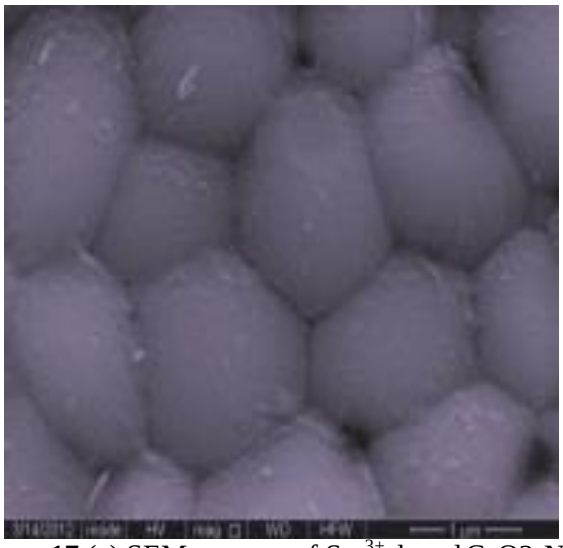

Figure 17 (a) SEM patterns of Sm^{3+} doped CeO2-NPs

Table 4 (a) and Figure 17 (a) illustrates shows the example calculation of Sm^{3+} doped CeO_2 nanoparticles crystallite size in SEM image. Let us consider 10 spheres in the SEM image. For each image diameter is calculated. Then the average of 10 spheres is obtained as 54.6nm. This is the final CeO_2 nanoparticles crystallite size in SEM image.

Table 4 (b) Example calculation of Ag doped CeO_2 nanoparticles crystallite size

Number of spheres in SEM image	Diameter of sphere in SEM image (nm)
1	45
2	65
3	76
4	63
5	74
6	62
7	85
8	82
9	63
10	84
11	85
12	83
13	82
14	75
15	92
Average mean	74.4

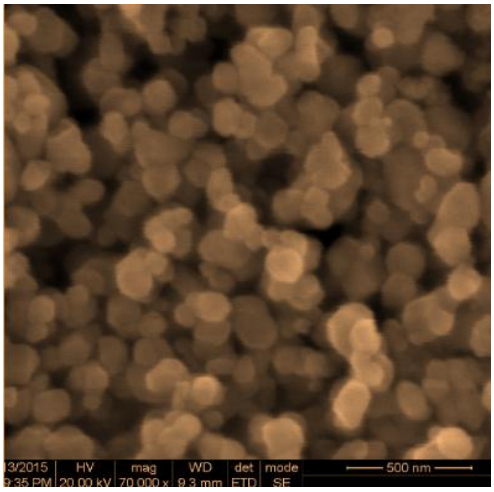

Figure 17 (b) SEM patterns of Ag doped CeO2-NPs

Table 4 (b)and Figure 17 (b) illustrates shows the example calculation of Ag doped CeO_2 nanoparticles crystallite size in SEM image. Let us consider 15spheres in the SEM image. For each image diameter is calculated. Then the average of 15 spheres is obtained as 74.4nm. This is the final CeO_2 nanoparticles crystallite size in SEM image

Table 4 (c) Example calculation of Eu doped CeO_2 nanoparticles crystallite size

Number of spheres in SEM image	Diameter of sphere in SEM image (nm)
1	40
2	55
3	63
4	55
5	41
6	52
7	57
8	63
9	55
10	63
11	71
12	72
13	58
14	62

15	69
16	47
17	56
18	85
19	96
20	45
Average mean	60.25

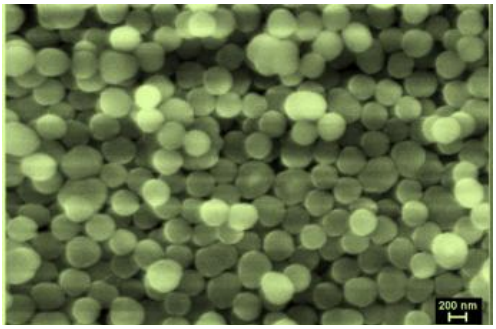

Figure 17 (c) SEM patterns of Eu doped CeO2-NPs

Table 4 (c) and Figure 17 (c) illustrates shows the example calculation of Eu doped CeO_2 nanoparticles crystallite size in SEM image. Let us consider 20 spheres in the SEM image. For each image diameter is calculated. Then the average of 20 spheres is obtained as 60.25nm. This is the final CeO_2 nanoparticles crystallite size in SEM image

4.6 Transmission Electron Microscopy (TEM)

The TEM characterization of doped CeO2-NPs is used to analyze the shape, size, and morphology. As shown in the figure, the nanoparticles are observed as spherical and pseudo-spherical in shape. By applying a TEM characterization, the CeO_2 nanoparticles crystallite size is analyzed with hexagonal structure. For each structure in the image, the surface area is calculated as given below,

$$Area = \frac{3\sqrt{3}}{2}\ a^2 \quad (8)$$

Where, $Area$ denotes a surface area of the hexagonal structure, a denotes a side of the structure. It is measured in nanometer (nm).

Table 5 Example calculation of CeO_2 nanoparticles crystallite size in TEM image

Number of hexagons in TEM image	**Area (nm) using Sm^{3+} doped CeO_2**	**Area (nm) using Ag doped CeO_2**	**Area (nm) using Eu doped CeO_2**
1	25.5	23.6	22.6
2	23.6	22.3	25.6
3	22.1	24	32.2
4	20.2	25.2	20.2
5	19.3	20.2	21.2
6	22.2	18.5	20.5
7	25.2	16.5	15.6
8	20.2	15.2	18.6
9	20.2	17.5	19.5
10	17.6	18.2	20.6
11	18.5	20.2	17.6
12	14.5	20.3	16.5
13	18.6	25.5	20.3
14	18.6	18.6	18.5
15	15.3	20.2	15.6
Average mean	**20.10**	**20.4**	**20.34**

Table 5 shows the example calculation of doped CeO_2 nanoparticles crystallite size in TEM image. Let us consider 15 hexagons in the TEM image. For each image, surface area of the length of the hexagon structure is calculated. Finally, the average is taken for 15 areas is 20nm. This is the final CeO_2 nanoparticles crystallite size in TEM image.

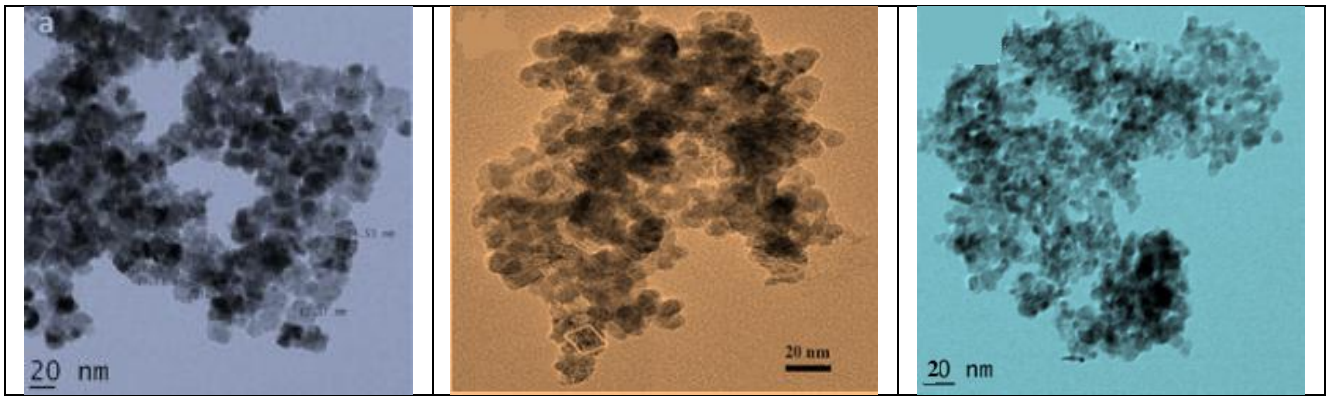

(a) **(b)** **(c)**

Figure 18 TEM patterns of (a) Sm^{3+} doped CeO_2 (b) Ag doped CeO_2 (c) Eu doped CeO2-NPs

Figure 18 illustrates the TEM images of the doped CeO_2 nanoparticles. The 20 nm of doped CeO_2 sizes with the results of TEM analysis are observed.

4.7 Field emission scanning electron microscopy (FE-SEM)

Field emission scanning electron microscopy (FE-SEM) is an advanced technology used to capture the microstructure image of the doped CeO_2 nanoparticles. This helps to used to analyze the CeO_2 nanoparticles size and shape.

In order to calculate the doped CeO_2-NPs particle with spherical structure using FE-SEM assessment, first the diameters of the spheres is measured based on the surface area of the particles.

$$D = 2 * \sqrt{\frac{Area}{\pi}} \qquad (9)$$

Where, D denotes a diameter of the particle in nanometer. After that, average of all the particles are considered as final size of the nanoparticles

Table 6 Example calculation of CeO_2 nanoparticles crystallite size in FE-SEM image

Number of Spheres in FE-SEM image	Diameter (nm) using Sm^{3+} doped CeO_2	Diameter (nm) using Ag doped CeO_2	Diameter (nm) using Eu doped CeO_2
1	99.5	95.6	102.3
2	100	105.3	112.2
3	99.6	95.6	106.2
4	98.8	85.3	84
5	99.6	102.2	105
6	99.8	104	65
7	98.7	112.2	74
8	108	85	101
9	92	97	115
10	99.2	63	125
11	85	85	143
12	110	98	125
13	99.5	102	85
14	115	125	62
15	99.8	145	96
Average mean	**100.3**	**100.01**	**100.05**

Table 6 shows the example calculation of doped CeO_2 nanoparticles crystallite size in FE-SEM image. Let us consider 15 spheres in the FE-SEM image. For each image, diameter of the length of the spheres structure is calculated. Finally the average is taken for 15 spheres is approximately 100nm. This is the final CeO_2 nanoparticles crystallite size in FE-SEM image.

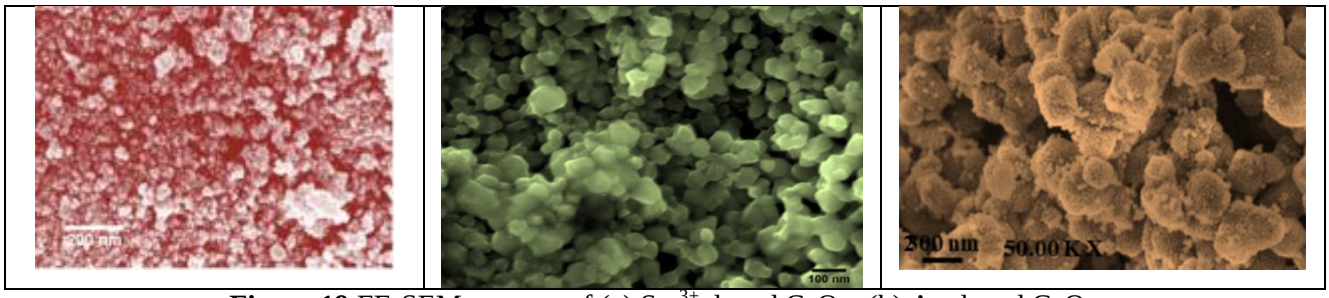

Figure 19 FE-SEM patterns of (a) Sm^{3+} doped CeO_2 (b) Ag doped CeO_2 (c) Eu doped CeO2-NPs

Figure 19 illustrates the TEM images of the doped CeO_2 nanoparticles. The 100 nm of doped CeO_2 sizes with the results of FE-SEM analysis are observed.

4.8 X-ray photoelectron spectroscopy (XPS)

XPS spectra are achieved by irradiating a solid surface with a beam of X-rays and calculating the kinetic energy of electrons that are emitted from the doped CeO_2 nanoparticles. XPS is a family of photoemission spectroscopy in which electron population spectra are recorded by irradiating a material with a beam of X-rays.

The binding energy of emitted electrons is computed by using the photoelectric effect equation,

$$e_{bind} = e_{ph} - (e_{kin} + \varphi) \quad (10)$$

Where, e_{bind} denotes a binding energy of the electron, e_{ph} indicates a energy of the X-ray photons, e_{kin} indicates a kinetic energy of the electron, term 'φ' represents the specific surface of the material,

Table 7 Performance of XPS with intensity versus binding energy

Binding energy (eV)	Intensity (a.u)		
	Sm^{3+} doped CeO_2	Ag doped CeO_2	Eu doped CeO_2
528	4850	2500	2500
530	10500	10000	3000
532	4800	9000	7500
534	4800	4900	5500
536	4800	4900	4900

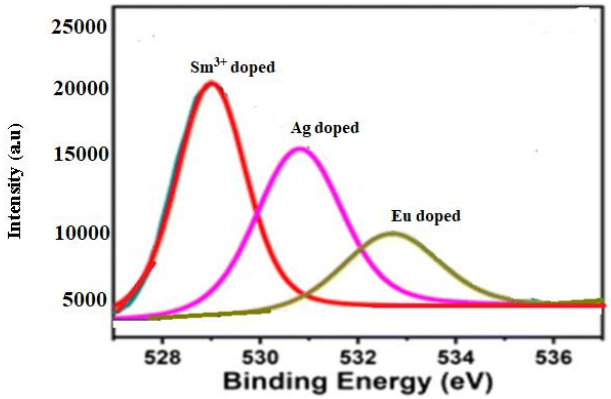

Figure 20 XPS spectra of (a) Sm^{3+} doped CeO_2 (b) Ag doped CeO_2 (c) Eu doped CeO2-NPs

Figure 20 reveals the performance of XPS spectra using doped CeO_2-NPs. As shown in the above graph, the vertical axis represents intensity in absorption unit (a.u) and the horizontal axis represents the binding energy in electron volt (eV). As shown in the graph, the intensity value of the Sm^{3+} doped CeO_2, Ag doped CeO_2, Eu doped CeO_2 and are represented by red color, pink color, and green color respectively.

4.9 Performance of concentration of doped ceo2 versus inhibition

Percentage of inhibition is measured based on the concentration of the doped CeO_2 nanoparticles.

Table 8 Performance of XPS with intensity versus binding energy

Concentration of doped ceo_2 (µg/mL)	Percentage of inhibition		
	Sm^{3+} doped CeO_2,	Ag doped CeO_2,	Eu doped CeO_2,
0.5	8	10	12
1	10	14	16
1.5	20	22	30
2	30	34	40
2.5	40	46	50
3	50	60	64

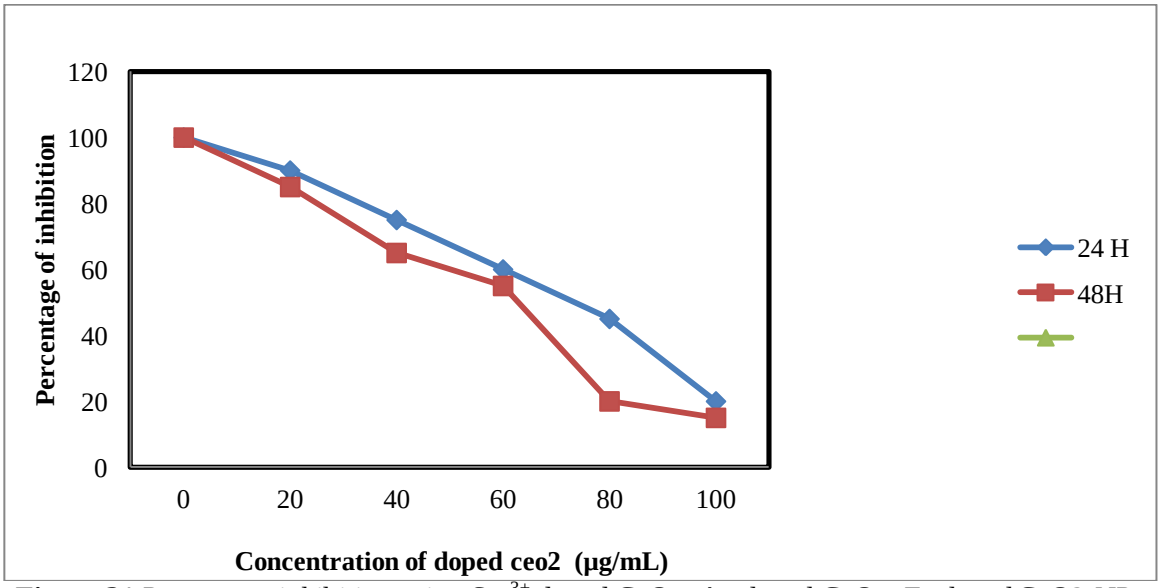

Figure 21 Percentage inhibition using Sm^{3+} doped CeO_2, Ag doped CeO_2 ,Eu doped CeO2-NPs

Figure 21 show graphs of percentage of inhibition in the Y axis and concentration of doped cerium oxide in X axis. The concentration of the doped cerium oxide is taken in the ranges from 0.5 µg/mL to 3 µg/mL Based on the input, the output of percentage inhibition is obtained.

4.10 Cell viability test by MTT assay

In present investigation, the Cell viability test by MTT assay effect of doped CeO_2 are examined in cultured (A549) human lung cancer cell line through revealing cells for 24 h and 48h.

Table 9 (a) Cell viability test using concentration of Sm^{3+} doped CeO_2

Concentration of Sm^{3+} doped CeO_2 (µg/ml)	Cell viability test (%)	
	24 H	48H
0	100	100
20	90	85
40	75	65
60	60	55
80	45	20
100	20	15

Table 9 (b) Cell viability test using concentration of Ag doped CeO_2

Concentration of Ag doped CeO_2 (µg/ml)	Cell viability test (%)	
	24 H	48H
0	100	100
20	70	85
40	75	65
60	60	55
80	45	20
100	30	25

Table 9 (c) Cell viability test using concentration of Eu doped CeO_2

Concentration of Eu doped CeO_2(µg/ml)	Cell viability test (%)	
	24 H	48H
0	100	100
20	85	75
40	70	60
60	50	40
80	35	20
25	20	18

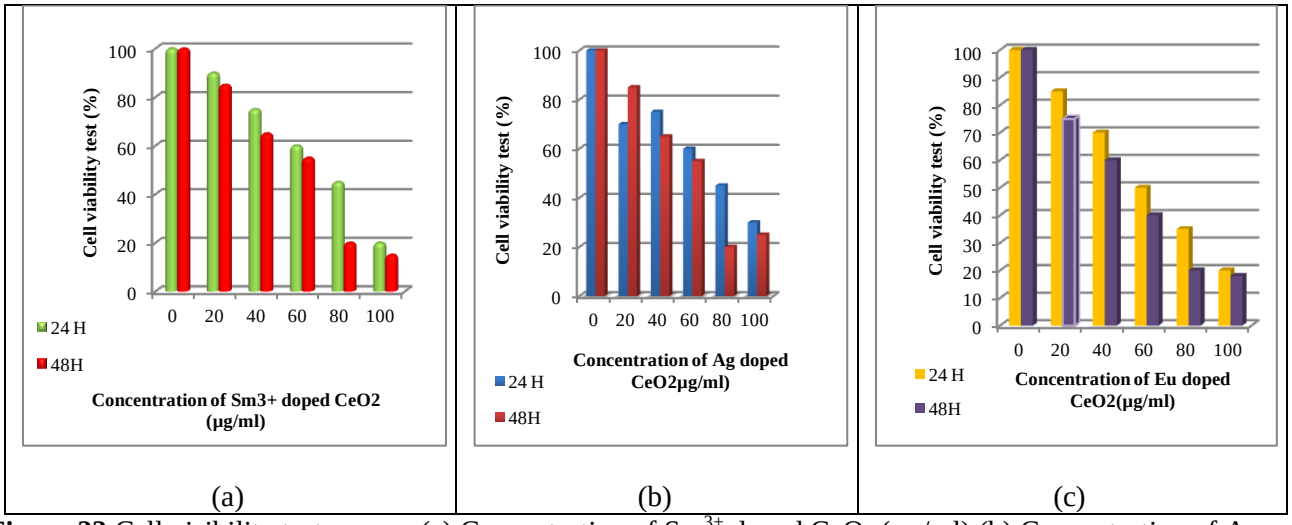

Figure 22 Cell visibility test versus (a) Concentration of Sm^{3+} doped CeO_2 (µg/ml) (b) Concentration of Ag doped CeO_2(µg/ml) (c) Concentration of Eu doped CeO_2(µg/ml)

As shown in Figure 22, the cancer cell viability are analyzed with respect with respect to different dopants nanoparticles concentration such as Sm^{3+} doped CeO_2**,** Ag doped CeO_2, Eu doped CeO_2. The concentration of dopants nanoparticles are taken in the ranges from 0, 20, 40...100 (**µg/ml).** The cancer cell viability are decreased partially with increasing the concentration of dopants **CeO_2** nanoparticles. The results show the direct dose-response relationship with tested cells only at higher concentrations.

4.11 Evaluation of anticancer activity of colony-forming assay

According to the colony-forming assay, dopants **CeO_2** nanoparticles are efficient at low concentrations. The anticancer activity is evaluated against three different screened and tested lung cancer cell lines such as A549, H460, and H1299.

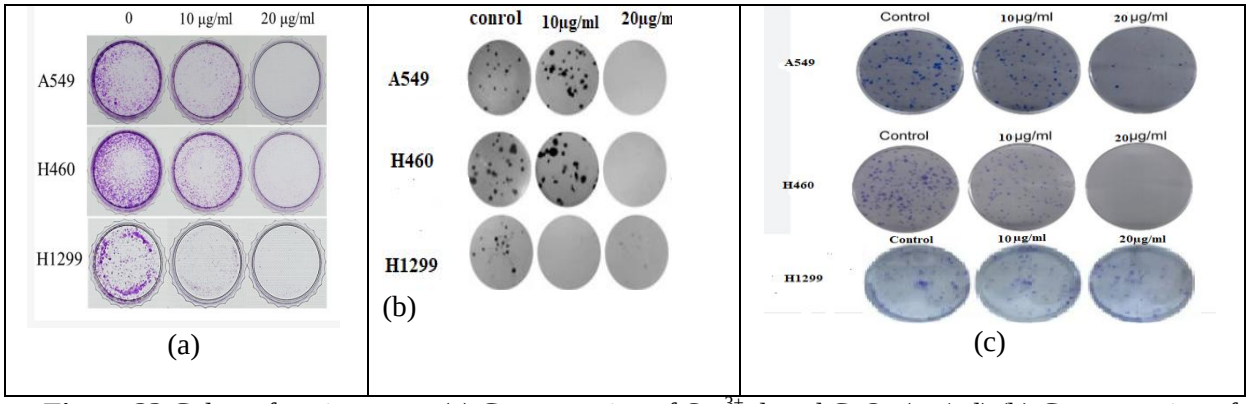

Figure 23 Colony-forming assay (a) Concentration of Sm^{3+} doped CeO_2 (µg/ml) (b) Concentration of Ag doped CeO_2(µg/ml) (c) Concentration of Eu doped CeO_2(µg/ml)

Figure 23 illustrates the colony-forming assay for three dopant **CeO_2** nanoparticles. The figure illustrates the anticancer activity of dopant **CeO_2** nanoparticles. The molecule clearly illustrated efficient inhibition of cell growth in a colony-forming assay at a low concentration. It means that the cancer cell lines are disappeared after treatment with 20 µg/ml of dopant **CeO_2** nanoparticles.

4.12 GCMS analysis of leaf extracts Indigoferra tinctoria and Centella Asiatica

A Gas chromatography mass spectrum (GCMS) analysis is carried out to determine the phytochemicals present in the aqueous extracts of the leaves such as Centella Asiatica and Indigoferra tinctoria.

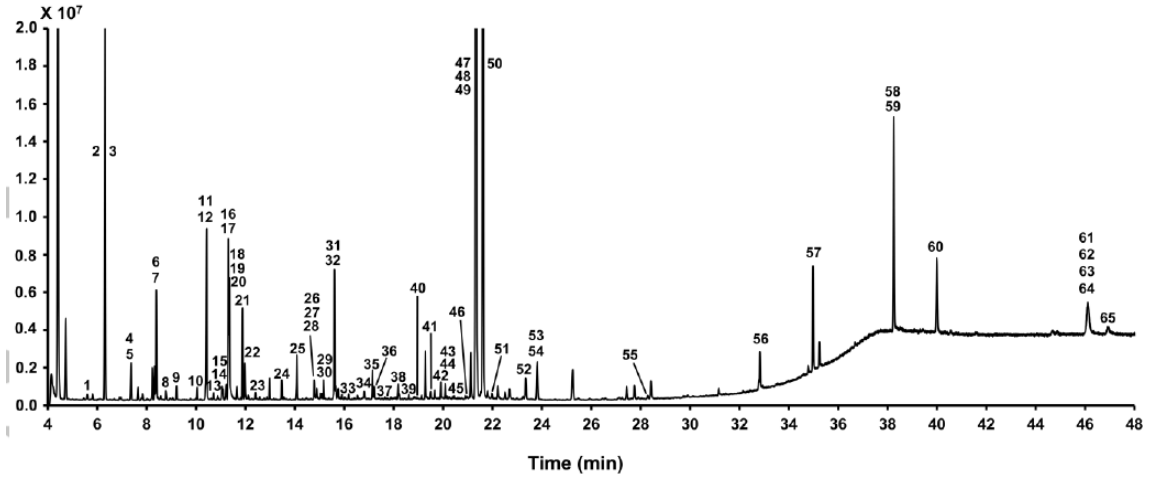

1. 2-Hydroxypyridine
2. Lactic acid
3. 2-Hydroxybutanoic acid
4. Creatine
5. Sarcosine
6. 3-Hydroxynorvaline
7. 2-Ketobutyric acid
8. Beta-hydroxybutyric acid
9. Carnitine
10. Valine
11. Glycocyamine
12. Urea
13. DL-dihydrosphingosine
14. Noradrenaline
15. Norleucine
16. Phosphate
17. Glycerol
18. Isoleucine
19. L-allothreonine
20. Proline
21. Glycine
22. Succinic acid
23. Fumaric acid
24. Threonine
25. 5-Aminovaleric acid
26. Nicotinamide
27. Malonic acid
28. Iminodiacetic acid
29. Malic acid
30. Methionine
31. Oxoproline
32. 5-Methoxyindole-3-acetic acid
33. L-cysteine
34. D-alanine-D-alanine
35. Glutamate
36. Phenylalanine
37. Taurine
38. Ribose
39. Xylitol
40. Pipecolinic acid
41. Hypoxanthine
42. Ornithine
43. Hippuric acid
44. Myristic acid
45. Tyrosine
46. Lyxose
47. Glucose
48. Talose
49. Lysine
50. L-DOPA
51. Mannitol
52. Palmitic acid
53. Cysteine-glycine
54. D-erythro-sphingosine
55. Spermidine
56. Inosine
57. Sedoheptulose
58. Alizarin
59. Cholesterol
60. Thymine
61. Phytosphingosine
62. Glucose-1-phosphate
63. Maltotriose
64. Beta-mannosylglycerat
65. Thymol

Figure 24 (a) GCMS analysis using leaf extracts Centella Asiatica

Figure 24 (a) Illustrates the GCMS analysis of using leaf extracts using Centella Asiatica medicinal herb. GC-MS of the ethanolic extract of the leaves of Indigofera tinctoria is carried out to determine the phytochemicals present in the extract is based on peak area, molecular weight and molecular formula.

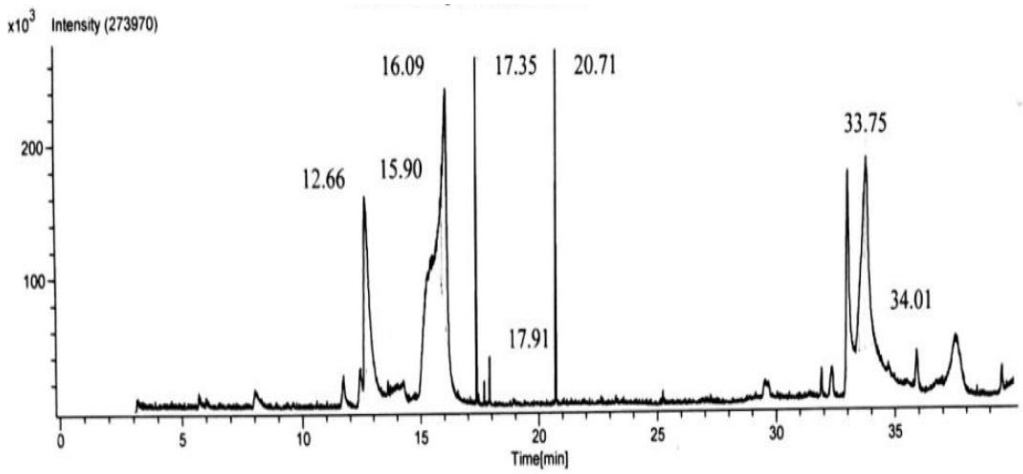

Figure 24 (b) GCMS analysis using leaf extracts Centella Asiatica

Peak Number	Time [min]	Type	Peak Width(FWH [min]	Area [Intens. * sec]	Height	Description	Start Point Time[min]	Start Point Height	End Point Time[min]	End Point Height
1	12.66	BV	0.0816	666881.58	137242.10		12.55	15724	12.68	28613
2	12.68	VB	0.1332	957257.87	130747.96		12.68	28613	12.93	52464
3	15.88	BV	0.1693	364913.64	67271.26		15.71	125413	15.88	94655
4	15.90	VV	0.0333	150785.47	80023.30		15.88	94655	15.92	88743
5	16.06	VV	0.1599	1270258.26	175333.84		15.92	88743	16.08	60353
6	16.09	VB	0.0576	758914.67	186637.14		16.08	60353	16.26	28418
7	17.35	BB	0.0268	443920.06	263423.51		17.31	4124	17.40	5306
8	17.91	BB	0.0236	59677.57	37063.65		17.86	4696	17.96	3013
9	20.71	BB	0.0284	484973.42	269842.06		20.67	3794	20.77	4509
10	32.98	BB	0.1090	961615.34	144978.05		32.86	9096	33.11	61863
11	33.46	BV	0.0589	146342.26	34901.45		33.32	39542	33.46	40835
12	33.70	VV	0.1696	1220517.90	128207.18		33.46	40835	33.71	43011
13	33.75	VV	0.1607	1501686.97	145940.66		33.71	43011	34.01	45656
14	34.01	VB	0.0525	77369.04	20500.71		34.01	45656	34.14	46832

Figure 24 (b) GCMS analysis using leaf extracts Indigofera tinctoria

Figure 24 (b) presences of numerous phyto-components in the aqueous extract of the leaves of Indigofera tinctoria. There are eight phyto-components are presented and the molecular formula are shown in the below table.

Table 10 Phyto-components of GCMS analysis using Indigoferra tinctoria

Sl. No.	Name of the phytochemical detected	Molecular Formula
1	2H-Indol-2-one, 1,3-dihydro-	C_8H_7NO
2	Myo-Inositol, 4-C-methyl-	$C_7H_{14}O_6$
3	Myo-Inositol, 2-C-methyl-	$C_7H_{14}O_6$
4	3,7,11,15-tetramethyl-2-hexadecen-1-ol	$C_{20}H_{40}O$
5	Pentadecanal-	$C_{15}H_{30}O$
6	Phytol	$C_{20}H_{40}O$
7	Benzoxazole, 2-methyl-	C_8H_7NO
8	1,2-Benzenediol, o- (2-bromopropionyl)-o'-(4-ethylbenzoyl)-	$C_{18}H_{17}BrO_4$

4.13 LC–MS analysis of leaf extracts using Centella Asiatica and Indigoferra tinctoria

Liquid chromatography-mass spectrometry (LC–MS) is a powerful analytical method and it employed for separation, detection, and quantification of both unknown and known compounds and also used to illuminate the structure and chemical properties of various molecules.

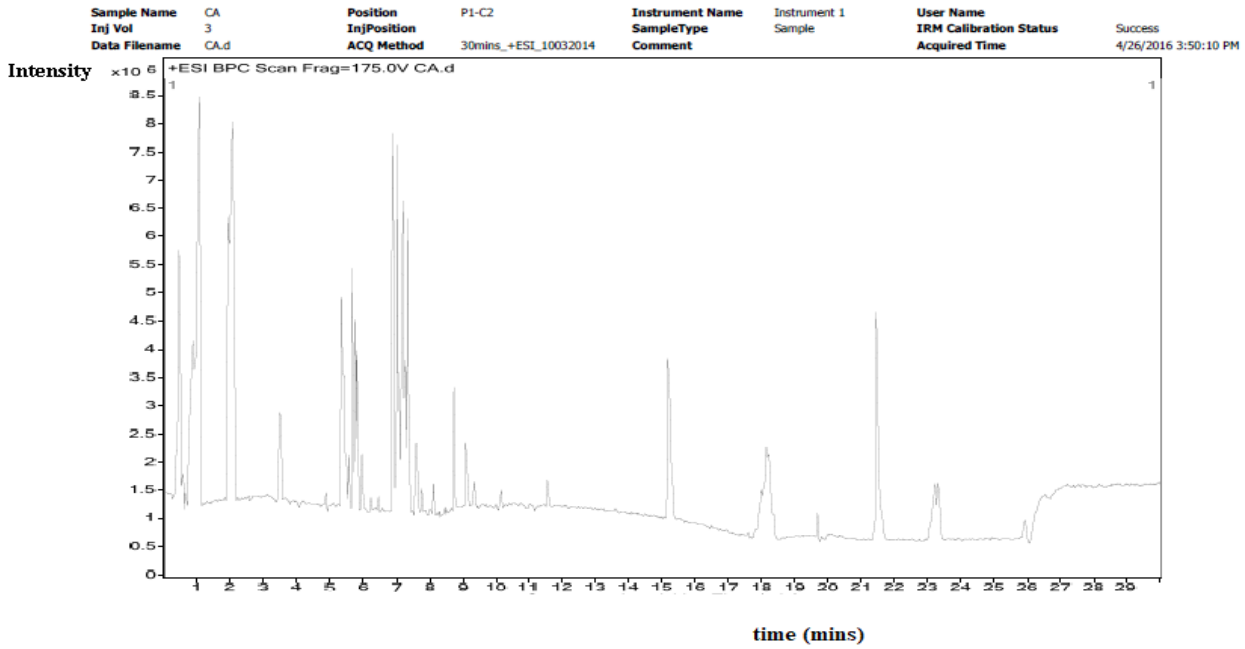

Figure 25(a) LC–MS using Centella Asiatica

Table 11 Qualitative Compound Report of LC–MS using Centella Asiatica

Compound Table

Compound Label	RT	Mass	Name	Formula	MFG Formula	DB Formula	DB Diff (ppm)	Hits (DB)
Cpd 1: 0.379	0.379	141.9926						
Cpd 2: Choline	0.493	104.1062	Choline	C5 H14 N O	C5 H14 N O	C5 H14 N O	12.87	2
Cpd 3: Trolamine	0.549	149.1037	Trolamine	C6 H15 N O3	C6 H15 N O3	C6 H15 N O3	10.17	6
Cpd 4: O-Acetylserine	0.676	147.0516	O-Acetylserine	C5 H9 N O4	C5 H9 N O4	C5 H9 N O4	10.86	10
Cpd 5: Trolamine	0.756	149.1035	Trolamine	C6 H15 N O3	C6 H15 N O3	C6 H15 N O3	11.52	6
Cpd 6: Neuraminic acid	0.789	267.0942	Neuraminic acid	C9 H17 N O8	C9 H17 N O8	C9 H17 N O8	4.69	9
Cpd 7: 4-Hydroxy-L-threonine	0.798	135.053	4-Hydroxy-L-threonine	C4 H9 N O4	C4 H9 N O4	C4 H9 N O4	0.95	3
Cpd 8: Guanine	0.836	151.0475	Guanine	C5 H5 N5 O	C5 H5 N5 O	C5 H5 N5 O	12.35	3
Cpd 9: nn-Dimethylaniline-n-oxide	0.84	138.0904	nn-Dimethylaniline-n-oxide	C8 H12 N O	C8 H12 N O	C8 H12 N O	11.08	6
Cpd 10: 1-Aminocyclohexanecarboxylic ...	0.842	143.0951	1-Aminocyclohexanecarboxylic ...	C7 H13 N O2	C7 H13 N O2	C7 H13 N O2	-3.49	13
Cpd 11: nn-Dimethylaniline-n-oxide	1.065	138.0904	nn-Dimethylaniline-n-oxide	C8 H12 N O	C8 H12 N O	C8 H12 N O	10.87	6
Cpd 12: Normetanephrine	1.065	183.0876	Normetanephrine	C9 H13 N O3	C9 H13 N O3	C9 H13 N O3	10.52	11
Cpd 13: Racepinephrine	2.028	183.0898	Racepinephrine	C9 H13 N O3	C9 H13 N O3	C9 H13 N O3	-1.38	15
Cpd 14: epsilon-Caprolactam	2.033	113.0848	epsilon-Caprolactam	C6 H11 N O	C6 H11 N O	C6 H11 N O	-6.86	8
Cpd 15: 4-aminohippurate	2.038	222.0981	4-aminohippurate	C11 H14 N2 O3	C11 H14 N2 O3	C11 H14 N2 O3	10.34	5
Cpd 16: Ethyl Oxalacetate	3.513	188.0666	Ethyl Oxalacetate	C8 H12 O5	C8 H12 O5	C8 H12 O5	9.85	4
Cpd 17: 4,6-dioxoheptanoic acid	4.903	158.0583	4,6-dioxoheptanoic acid	C7 H10 O4	C7 H10 O4	C7 H10 O4	-2.43	13
Cpd 18: 3-methyl-dodecanedioic acid	5.379	244.1673	3-methyl-dodecanedioic acid	C13 H24 O4	C13 H24 O4	C13 H24 O4	0.51	8
Cpd 19: Galactosylhydroxylysine	5.382	324.1519	Galactosylhydroxylysine	C12 H24 N2 O8	C12 H24 N2 O8	C12 H24 N2 O8	4.3	12
Cpd 20: N-Monodesmethyldiltiazem	5.99	400.1458	N-Monodesmethyldiltiazem	C21 H24 N2 O4 S	C21 H24 N2 O4 S	C21 H24 N2 O4 S	-0.42	15
Cpd 21: Ala Glu His	6.237	355.1512	Ala Glu His	C14 H21 N5 O6	C14 H21 N5 O6	C14 H21 N5 O6	-5.59	10
Cpd 22: Arg Gly Gly	6.472	288.1544	Arg Gly Gly	C10 H20 N6 O4	C10 H20 N6 O4	C10 H20 N6 O4	0.54	6

Cpd 46: 1alpha-hydroxy-24-(dimethylphosphoryl)-25,26,27-trinorvitamin D3 / 1alpha-hydroxy-24-(dimethylphosph	18.341	434.2958	1alpha-hydroxy-24-(dimethylphosphoryl)-25,26,27-trinorvitamin D3 / 1alpha-hydroxy-24-(dimethylphosph	C26 H43 O3 P	C26 H43 O3 P	C26 H43 O3 P	-1.91	15
Cpd 47: 3beta,6alpha,7alpha-Trihydroxy-5beta-cholan-24-oic Acid	21.481	408.2827	3beta,6alpha,7alpha-Trihydroxy-5beta-cholan-24-oic Acid	C24 H40 O5	C24 H40 O5	C24 H40 O5	11.91	15
Cpd 48: 23.154	23.154	512.3993						
Cpd 49: 23.228	23.228	446.3914						
Cpd 50: N'-5Z,8Z,11Z,14Z-eicosatetraenoyl-N''-diethyl-ethylenediamine	23.348	402.3656	N'-5Z,8Z,11Z,14Z-eicosatetraenoyl-N''-diethyl-ethylenediamine	C26 H46 N2 O	C26 H46 N2 O	C26 H46 N2 O	-11.45	1

Cpd 23: clavirin II	6.912	290.1467	clavirin II	C17 H22 O4	C17 H22 O4	C17 H22 O4	17.53	4
Cpd 24: 3-oxo-tridecanoic acid	7.035	228.1731	3-oxo-tridecanoic acid	C13 H24 O3	C13 H24 O3	C13 H24 O3	-2.23	15
Cpd 25: 10-keto tridecanoic acid	7.035	228.1724	10-keto tridecanoic acid	C13 H24 O3	C13 H24 O3	C13 H24 O3	0.58	7
Cpd 26: 1alpha,25-dihydroxy 26,27-dimethyl-20,21-didehydro-23-oxavitamin D3 / 1alpha,25-dihydroxy-26,27-dime	7.135	446.3376	1alpha,25-dihydroxy-26,27-dimethyl-20,21-didehydro-23-oxavitamin D3 / 1alpha,25-dihydroxy-26,27-dime	C28 H46 O4	C28 H46 O4	C28 H46 O4	4.55	15
Cpd 27: 7.142	7.142	991.527						
Cpd 28: 10-keto tridecanoic acid	7.202	228.1729	10-keto tridecanoic acid	C13 H24 O3	C13 H24 O3	C13 H24 O3	-1.47	7
Cpd 29: 10-keto tridecanoic acid	7.351	228.1727	10-keto tridecanoic acid	C13 H24 O3	C13 H24 O3	C13 H24 O3	-0.59	7
Cpd 30: Ergoline-8-methanol, 10-methoxy-6-methyl-, (8b)-	7.352	286.1753	Ergoline-8-methanol, 10-methoxy-6-methyl-, (8b)-	C17 H22 N2 O2	C17 H22 N2 O2	C17 H22 N2 O2	-24.93	1
Cpd 31: Typhasterol	7.621	448.3533	Typhasterol	C28 H48 O4	C28 H48 O4	C28 H48 O4	4.36	15
Cpd 32: 7.625	7.625	975.5325						
Cpd 33: GPSer(14:0/14:0)[U]	8.132	679.4468	GPSer(14:0/14:0)[U]	C34 H66 N O10 P	C34 H66 N O10 P	C34 H66 N O10 P	-6.43	2
Cpd 34: 8.477	8.477	360.2839						
Cpd 35: dihydroergocornine	9.127	563.3116	dihydroergocornine	C31 H41 N5 O5	C31 H41 N5 O5	C31 H41 N5 O5	-1.45	5
Cpd 36: PGF1a alcohol	10.165	342.2842	PGF1a alcohol	C20 H38 O4	C20 H38 O4	C20 H38 O4	-21.07	5
Cpd 37: 8alpha-3beta-hydroxy-estra-1,3,5(10)-trien-17-one	11.569	270.1622	8alpha-3beta-hydroxy-estra-1,3,5(10)-trien-17-one	C18 H22 O2	C18 H22 O2	C18 H22 O2	-0.66	6
Cpd 38: Lactone of PGF-MUM	15.218	296.1589	Lactone of PGF-MUM	C16 H24 O5	C16 H24 O5	C16 H24 O5	11.68	3
Cpd 39: 17.970	17.97	482.3547						
Cpd 40: 17.974	17.974	499.3813						
Cpd 41: 18.094	18.094	543.4072						
Cpd 42: 18.102	18.102	526.3807						
Cpd 43: 18.172	18.172	482.3547						
Cpd 44: 18.179	18.179	499.3814						
Cpd 45: 27-nor-5b-cholestane-3a,7a,12a,24,25-pentol	18.186	438.329	27-nor-5b-cholestane-3a,7a,12a,24,25-pentol	C26 H46 O5	C26 H46 O5	C26 H46 O5	12.52	1

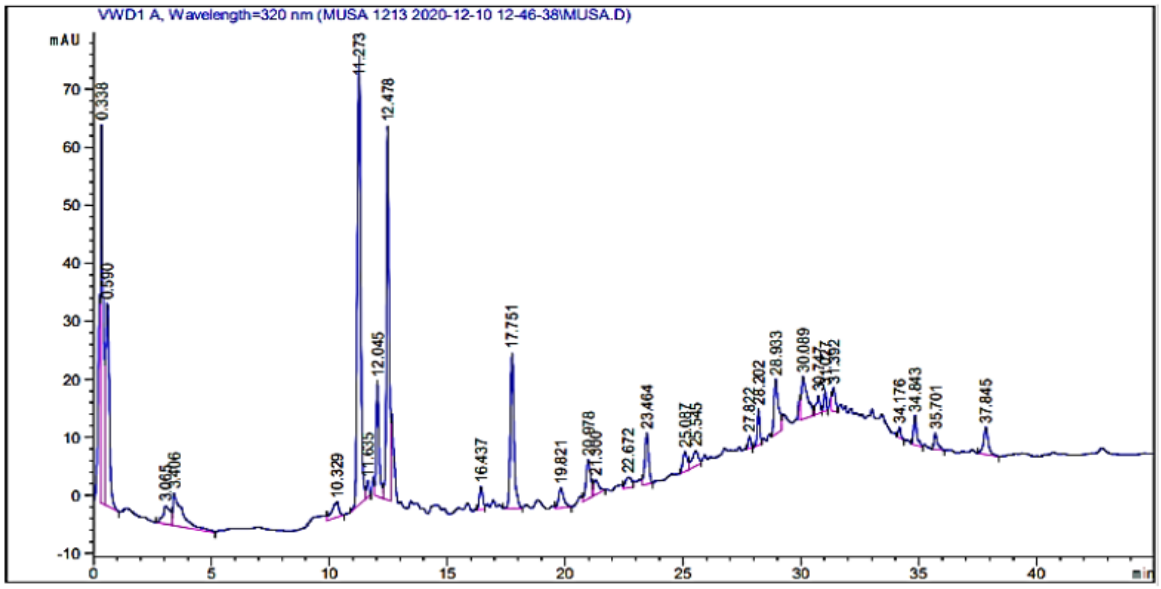

Figure 25(b) LC–MS using Indigoferra tinctoria

Figure 25 (b) indicates a Liquid chromatography-mass spectrometry (LC–MS) of plant extract from Indigoferra tinctoria. This analysis is used for identifying the structure and phytochemical Compounds reports of various molecules as shown in table 11 (b).

Table 11 (b) Qualitative Compound Report of LC–MS using Indigoferra tinctoria

Retention Time (RT) (min)	Phytochemical Compounds	Sample Peak Area
10.329	Mandelic acid	55.548
11.273	Bis-HHDP-hex(pedunculagin)	797.264
12.478	Caffeic acid	510.522
16.437	Hydroxy bezoic acid	38.4805
20.978	Chlorogenic acid	91.0721
22.672	Morin	32.6104
23.464	Syringic acid	100.907
25.087	5-0-dicaffeoylquinic acid	42.0698
25.545	Kaempferol-3-(caffeoyl-diglucoside)-7-rhamnosyl	50.79067
27.822	Kaempferol-3-(p-coumaroyl-diglucoside)- 7-glucoside	15.8819
30.089	Quercetin	131.189
31.027	Qurcetin-3-(caffeoyldiglucoside)-7-glucoside	24.0199
34.843	Quercitin-3-O-rutinoside	47.3937
37.845	Glucose	4.6713

5. Conclusion

In this paper, antimicrobial activity of doped CeO_2 nanoparticles using agar disc-diffusion antibiotic susceptibility method is developed for estimating the effect of antibacterial and antifungal. Antimicrobial activity analyses used to resist or slow the spread of microorganisms. Microorganisms include bacteria and fungus in biomedical applications. First, the agar disc-diffusion antibiotic susceptibility method is introduced for identifying the antimicrobial characteristics of the doped CeO_2 nanoparticles and identifying the antibiotic-resistance profile pattern based on inhibition zone. After that, the photoluminescence intensity of gamma radiation dosimeter is measured to improve the optical and optoelectronic performance of the doped CeO_2. Finally, thermoluminescence intensity method is developed for gamma radiation dosimeter of the CeO_2 nanoparticles with respect to different temperatures. Finally, the anticancer activity analyses of doped CeO_2 used to resist the spread of cancer cells through the MTT assay. The performance analysis indicates that the antimicrobial effects of doped CeO_2 nanoparticles is improved and also increased the photoluminescence intensity, thermoluminescence intensity, SEM, TEM, XPS, XRD, FE SEM, values of gamma radiation dosimeter applications. In addition, anticancer effects of doped CeO_2

nanoparticles is improved in terms of Cell viability test , anticancer activity of colony-forming assay, GCMS analysis and LC–MS analysis.

References

1. Gusliani Eka Putri, Yetria Rilda, Syukri Syukri, Arniati Labanni, Syukri Arief, "Highly antimicrobial activity of cerium oxide nanoparticles synthesized using Moringa oleifera leaf extract by a rapid green precipitation method", Journal of Materials Research and Technology, Elsevier, Volume 15, 2021, Pages 2355-2364. https://doi.org/10.1016/j.jmrt.2021.09.075
2. F.T. Thema, D. Letsholathebe, K. Mphale, "Enhanced antibacterial properties of green synthesized nano ceria via Agathosma betulina natural extract", Materials Today: Proceedings, Elsevier, Volume 36, 2021, Pages 435-439. https://doi.org/10.1016/j.matpr.2020.05.010
   Helen Merina Albert, T. Lohitha, Karthik Alagarsamy, C.Alosious Gonsago, Vinita Vishwakarma, "Performance of ZnSO4 doped CeO2 nanoparticles and their antibacterial mechanism", Materials Today: Proceedings, Elsevier, Volume 47, 2021, Pages 1030-1034. https://doi.org/10.1016/j.matpr.2021.06.124
3. Mushtaq A. Dar, Rukhsana Gul, Ponmurugan Karuppiah, Naif A. Al-Dhabi, and Assim A. Alfadda , "Antibacterial Activity of Cerium Oxide Nanoparticles against ESKAPE Pathogens", Crystals, Volume 12, Issue 2, Pages 1-10. https://doi.org/10.3390/cryst12020179
4. Khosro Zamani, Noushin Allah-Bakhshi, Faezeh Akhavan, Mahdieh Yousefi, Rezvan Golmoradi, Moazzameh Ramezani, Horacio Bach, Shabnam Razavi, Gholam-Reza Irajian, Mahyar Gerami, Ali Pakdin-Parizi, Majid Tafrihi & Fatemeh Ramezani, "Antibacterial effect of cerium oxide nanoparticle against Pseudomonas aeruginosa", BMC Biotechnology, Springer, Volume 21, 2021, Pages 1-11. https://doi.org/10.1186/s12896-021-00727-1
5. Abbas Rahdar, Hamid Beyzaei, Faezeh Askari, George Z. Kyzas, "Gum-based cerium oxide nanoparticles for antimicrobial assay", Applied Physics, Springer, Volume 126, 2020, Pages 1-9. https://doi.org/10.1007/s00339-020-03507-4
6. Emilia Barker, Joanna Shepherd and Ilida Ortega Asencio , "The Use of Cerium Compounds as Antimicrobials for Biomedical Applications" Molecules, Volume 27, 2022, Pages 1-23. https://doi.org/10.3390/molecules27092678
7. Parisa Maleki, Fahimeh Nemati, Aida Gholoobi, Alireza Hashemzadeh, Zahra Sabouri, Majid Darroudi, "Green facile synthesis of silver-doped cerium oxide nanoparticles and investigation of their cytotoxicity and antibacterial activity", Inorganic Chemistry Communications, Elsevier, Volume 131, 2021, Pages 1-9. https://doi.org/10.1016/j.inoche.2021.108762
8. Oana L. Pop, Amalia Mesaros, Dan C. Vodnar, Ramona Suharosch, Flaviu Tabaran, Lidia Magerus, István Sz. Tódor , Zori¸ta Diaconeasa, Adriana Balint, Lelia Ciontea and Carmen Socaciu, "Cerium Oxide Nanoparticles and Their Efficient Antibacterial Application In Vitro against Gram-Positive and Gram-Negative Pathogens", Nanomaterials, Volume 10, Issue 8, Pages 1-15. https://doi.org/10.3390/nano10081614
9. A. Balamurugan, M. Sudha, S. Surendhiran, R. Anandarasu, S. Ravikumar, Y.A. Syed Khadar, "Hydrothermal synthesis of samarium (Sm) doped cerium oxide (CeO2) nanoparticles: Characterization and antibacterial activity", Materials Today: Proceedings, Elsevier, Volume 26, 2020, Pages 3588-3594. https://doi.org/10.1016/j.matpr.2019.08.217
10. Shalendra Kumar, Faheem Ahmed, Nagih M. Shaalan and Osama Saber, "Biosynthesis of CeO2 Nanoparticles Using Egg White and Their Antibacterial and Antibiofilm Properties on Clinical Isolates", Crystals, Volume 11, Issue 6, 2021, Pages 1-12. **https://doi.org/10.3390/cryst11060584**
11. N Sanjana Devi, Dhanraj M. Ganapathy, S Rajeshkumar, and Subhabrata Maiti, "Characterization and antimicrobial activity of cerium oxide nanoparticles synthesized using neem and ginger", Journal of Advanced Pharmaceutical Technology & Research | Volume 13, 2022, Pages S491–S495. doi: 10.4103/japtr.japtr_196_22
12. Shama Sehar, Iffat Naz, Abdul Rehman, Wuyang Sun, Saleh S. Alhewairini, Muhammad Nauman Zahid, Adnan Younis, "Shape-controlled synthesis of cerium oxide nanoparticles for efficient dye photodegradation and antibacterial activities", Applied Organometallic Chemistry, Wiley, Volume 35, Issue1, 2021, Pages 1-10. https://doi.org/10.1002/aoc.6069

13. Stefano Raimondi, Alfonso Zambo, Raffaella Ranieri, Francesca Fraulini, Alberto Amaretti, Maddalena Rossi, Gigliola Lusvardi, "Investigation on the antimicrobial properties of cerium-doped boactive glasses", Journal of Biomedical Material Research, Wiley, Volume 110, Issue 2, 2022, Pages 504-508. https://doi.org/10.1002/jbm.a.37289
14. Suhad A. Abid & Ali A. Taha & Raid A. Ismail & Mayyadah H. Mohsin, "Antibacterial and cytotoxic activities of cerium oxide nanoparticles prepared by laser ablation in liquid", Environmental Science and Pollution Research, Springer, Volume 27, 2020, Pages 30479–30489. https://doi.org/10.1007/s11356-020-09332-9
15. Isabela A.P. Farias , Carlos C.L. Santos, Aline L. Xavier, Tatianne M. Batista, Yuri M. Nascimento, Jocianelle M.F.F. Nunes, Patrı´cia M.F. Silva, Raimundo A. Menezes-Ju´nior, Jailson M. Ferreira, Edeltrudes O. Lima, Josean F. Tavares, Marianna V. Sobral, Dawy Keyson ,Fa´bio C. Sampaio, "Synthesis, physico- chemical characterization, antifungal activity and toxicological features of cerium oxide nanoparticles", Arabian Journal of Chemistry, Elsevier, Volume 14, Issue 1, 2021, Pages 1-14. https://doi.org/10.1016/j.arabjc.2020.10.035
16. Awais Ahmad, Muhammad Sufyan Javed, Safia Khan, Tahani Mazyad Almutair, Abdallah A.A. Mohammed, Rafael Luque, "Green synthesized Ag decorated CeO2 nanoparticles: Efficient photocatalysts and potential antibacterial agents", Chemosphere, Elsevier, Volume 310, 2023, Pages 1-10. https://doi.org/10.1016/j.chemosphere.2022.136841
17. Naheed Zafara, Bushra Uzaira, Muhammad Bilal Khan Niazib , Farid Menaac, Ghufrana Samind , Barkat Ali Khane , Haroon Iqbalf , Bouzid Menaa, "Green Synthesis of Ciprofloxacin-Loaded Cerium Oxide/Chitosan Nanocarrier and its Activity Against MRSA-Induced Mastitis", Journal of Pharmaceutical Sciences, Elsevier, Volume 110, Issue 10, 2021, Pages 3471-3483. https://doi.org/10.1016/j.xphs.2021.06.017
18. S. Gnanam , J. Gajendiran, J. Ramana Ramya, K. Ramachandran, S. Gokul Raj, "Glycine-assisted hydrothermal synthesis of pure and europium doped CeO2 nanoparticles and their structural, optical, photoluminescence, photocatalytic and antibacterial properties", Chemical Physics Letters, Elsevier, Volume 763, 2021, Pages 1-7. https://doi.org/10.1016/j.cplett.2020.138217
19. S. Aldawood, M.S. AlGarawi, Muhammad Ali Shar, Syed Mansoor Ali, "Analysis of gamma dose dependent nanostructure, morphological, optical and electrical properties of CeO2 thin films", Journal of King Saud University – Science, Elsevier, Volume 32, Issue 5, 2020, Pages 2629-2634. https://doi.org/10.1016/j.jksus.2020.05.004